SELECTION OF OPTIMUM LATERAL LOAD-RESISTING SYSTEM USING ARTIFICIAL NEURAL NETWORKS

By

Eng. Maha Abu El-Makarem M. Badr El-Din

A Thesis Submitted to the
Faculty of Engineering at Cairo University
in Partial Fulfillment of the
Requirements for the Degree of
MASTER OF SCIENCE
in
STRUCTURAL ENGINEERING

Supervised by

Prof. Dr. Sherif A. Mourad	Dr. M.Hany El-Gammal	Dr. Magdy M.Wahba
Professor of Steel Structures and Bridges	Assistant Professor	Associate Professor
Structural Eng. Dept.	Structural Eng. Dept.	Structural Eng. Dept.
Faculty of Engineering	Faculty of Engineering	Faculty of Engineering
Cairo University	Cairo University	Cairo University

FACULTY OF ENGINEERING, CAIRO UNIVERSITY
GIZA, EGYPT
December 2006

SELECTION OF OPTIMUM LATERAL LOAD-RESISTING SYSTEM USING ARTIFICIAL NEURAL NETWORKS

By

Eng. Maha Abu El-Makarem M. Badr El-Din

A Thesis Submitted to the
Faculty of Engineering at Cairo University
in Partial Fulfillment of the
Requirements for the Degree of
MASTER OF SCIENCE
in

STRUCTURAL ENGINEERING

Approved by the
Examining Committee:

_____

Prof. Dr. Sherif Ahmed Mourad

_____

Prof. Dr. Abdelrahim Khalil Dessouki

_____

Prof. Dr. Mokhtar Mahmoud Seddeik

_____

FACULTY OF ENGINEERING, CAIRO UNIVERSITY
GIZA, EGYPT
December 2006

ACKNOWLEDGEMENTS

I thank God for providing me with the means to accomplish this research.

I am greatly indebted to Prof. Dr. Sherif Mourad, Professor of Steel Structures and Bridges, Structural Engineering Department, Faculty of Engineering, Cairo University, for his invaluable support and effort throughout the development of this thesis.

I would like to express my appreciation for Dr. Magdy Mourad, Associate Professor, Structural Engineering Department, Faculty of Engineering, Cairo University, for his concern, and great encouragement and support.

I am also grateful to Dr. Hany El-Gammal, Assistant Professor, Structural Engineering Department, Faculty of Engineering, Cairo University, for his new ideas, and fruitful discussions which helped in producing the thesis in its current form.

ABSTRACT

This study proposes an artificial neural network for the selection of optimal lateral load-resisting system for multi-story steel frames. The lateral load-resisting systems include rigid frames, braced frames and braced frames with outrigger truss. The frame parameters include the number of bays, the number of stories, in addition to the lateral load-resisting system. The frame design is based on both stress and deformation criteria under the load combinations of dead, live, and wind loads. The analysis is performed using a finite-element program whereas the design is implemented using MATLAB programs for the optimal design of sections. Several cycles of analysis and design are performed to achieve an optimum design for individual elements.

A neural network is then proposed in order to reduce the amount of computing time required in the numerous iterations involving structural analysis and design programs. A feed-forward backpropagation neural network is trained based on the results of the design of specific frame configurations. Input parameters for network define the frame configuration including number of bays, number of stories and the lateral load-resisting system, whereas the output parameters define the frame maximum lateral deformation and total weight. Different architectures of networks are studied to solve the problem. The accepted network is chosen based on the minimum value of the root-mean square error.

Table of Contents

List of Figures

List of Tables

List of Symbols and Abbreviations

A, a	: Output Vector
A_1	: Bending Stress Amplification Factor
AI	: Artificial Intelligence
ANN	: Artificial neural network
b	: Bias
Br	: Braced
BRFDES	: Braced Frame Design
c_m	: Equivalent Moment Factor
cm	: Centimeter
EI_c	: Overall Bending Stiffness of Exterior Columns
EI_o	: Bending Stiffness of Outrigger
EI_t	: Bending Stiffness of Frame
f	: Transfer Function
f_{bcx}	: Actual Compressive Bending Stress
F_{bcx}	: Allowable Compressive Bending Stress
F_c	: Allowable Compressive Axial Stress
f_{ca}	: Actual Compressive Axial Stress
F_{Ex}	: Euler Stress divided by a Factor of Safety
Fr	: Frame
F_y	: Yield Stress
GA_o	: Racking Shear Stiffness of Outriggers
GA_t	: Racking Shear Stiffness of Braced Frame
H	: Total Height of Frame
h	: Story Height
K	: Effective Length Factor
m	: Meter
M_r	: Restraining Moment
mse	: Mean Square Error
N	: Number of Floors
N	: Number of Training or Testing Sets
n	: Argument of Transfer Function

n	: Number of Braced Bays
OR	: Outrigger
ORFDES	: Outrigger Frame Design
P	: Input Vector
R	: Correlation Coefficient
R	: Number of Inputs
RGFDES	: Rigid Frame Design
RMSE	: Root-Mean Square Error
S	: Number of Neurons
T	: Target Vector
V	: Average Cumulative Shear Value per Floor
w	: Uniformly Distributed Lateral Load
W	: Weight Matrix
x	: Distance Measured from Top of Frame to the Mid Height of Outrigger

CHAPTER (1)

INTRODUCTION

1.1 PROBLEM STATEMENT

Any project is first established by the architect in conceptual terms, identifying the overall shape of the building, approximate number of floors, and the size and location of service cores. The main task for the structural engineer at this stage is to explore the structural options and to recommend a system that is not only satisfying all disciplines but is also cost efficient. The structural cost of multi-story steel buildings is the summation of the total tonnage of the steel used, and fabrication and erection costs. The steel fabrication and erection prices are mainly affected by the number and type of connections. It can be assumed that these costs remain the same for different structural steel schemes [1].

The design of a multi-story steel building under lateral loads is usually governed by system performance criteria (overall stiffness) rather than by component performance criteria (strength) [2]. Design comprises selecting and proportioning member sizes in which the stresses do not exceed the permissible values under any combination of loads, and the deformations meet applicable serviceability criteria. It is a challenging task for the structural designer, because it involves a large number of possibilities to achieve a selection satisfying design criteria while maintaining the least possible weight.

The problem then is in the excessive time consumed in the trial and error procedures to achieve a satisfactory solution within a tight duration.

1.2 THESIS OBJECTIVE AND METHODOLOGY

This study explores the feasibility of exploiting one of the artificial intelligence (AI) techniques to map rapidly the relation between the lateral load-resisting systems for multi-story steel frames and their expected lateral drift and optimum weight. The artificial neural networks (ANNs) are implemented for the derivation of this relation.

An artificial neural network is a class of computing device that operates in a manner analogous to that of the biological nervous system. It is an interconnected network of processing elements that has the ability to be trained to map a given input into the desired output [3]. If the training data are the analytical results for several configurations of lateral load-resisting frames, then the neural network gives to the structural designer the expected maximum lateral drift and optimum weight without repetitive trial-and-error procedures.

The methodology of this investigation is described as follows:

- First, the analysis of several multi-story steel frames with different configurations, and lateral load-resisting systems are performed to evaluate the expected lateral drift and optimum weight.
- Second, input and output data are prepared for training and testing the feed forward backpropagation neural network.
- Finally, the prepared data are then implemented in modeling the optimum artificial neural network architecture.

1.3 THESIS ORGANIZATION

The thesis is divided into five chapters organized as follows:

- Chapter one contains problem statement, thesis objective, methodology, and organization.
- Chapter two contains the literature review of the study which defines the design criteria of multi-story steel frames, and an overview about artificial neural networks.
- Chapter three introduces the chosen frame configurations, lateral systems, applied loads, design profiles, design codes and limitations for the multi-story frame analysis. It also presents the implemented analysis tools and the resulting lateral drifts and weights for the analyzed frames.
- Chapter four introduces the neural network model design including identification method for input parameters, and the performance of different network architectures.

- Chapter five includes a brief summary, conclusion and recommendations for possible future work.
- Annex (A) includes table of input and output data for training and testing the neural network.

CHAPTER (2)

LITERATURE REVIEW

2.1 OBJECTIVE

An overview on the basic concepts and fundamentals of the structural analysis of the selected lateral load-resisting systems, and the artificial neural network is discussed in this chapter.

2.2 DESIGN CRITERIA FOR LATERAL LOAD-RESISTING SYSTEMS

Structural analysis is a mathematical process by which the engineer computes the stresses and deformations for all elements of the structure under various loading conditions. Design is an iterative process in which chosen cross-sections are checked to ensure that they conform to the design limits of applicable codes. In this research the Egyptian Code of Practice for Steel Construction and Bridges [4] is used as the code of reference, and all members are chosen to comply with strength and serviceability limits defined by this code.

Strength Criteria

According to the Egyptian specifications, the design is based on the allowable stress design and on the assumptions of linear elastic theory. We highlight only the basic aspects for the design.

Girders:

Almost all floor beams are wide-flange shapes possessing an axis of symmetry about the plane of bending, and are designed to bend about the major axis. Lateral supports for flexural members are required because the compression flange behaves in a manner similar to a column and tends to buckle in the absence of lateral supports. In the design of steel beams, we can assume the existence of adequate lateral bracing constituted from the metal decking welded to the top flange at sufficient intervals, and from the cross beams connections to the beam flange.

Columns:

When a straight column is subjected to a combined bending and axial compressive stresses, the member behaves as a beam column. The Egyptian specifications give comprehensive rules for the elastic design of beam columns. The first step is to calculate the effective length of the column, which is expressed as *K* times the actual length. An "alignment chart" is provided to evaluate *K* when the elastic rotational restraints are known. For columns in frames which are free to sway, the designer is cautioned that the effective length can exceed twice the length of the column, and that the maximum slenderness ratio can't exceed 180.

The next step is to check the safety of the column by the use of interaction formulas. Moment magnification is negligible when axial load is small, a simple relation applicable only when $f_{ca}/F_c \leq 0.15$ is given. For bending in one plane, only this equation is of the form

$$\frac{f_{ca}}{F_c} + \frac{f_{bcx}}{F_{bcx}} \leq 1.0 \qquad (2.1)$$

where f_{ca} ,and f_{bcx} are the compressive axial and bending stresses, respectively at working loads; F_c is the allowable compressive axial stress, and F_{bcx} is the allowable compressive bending stress. When the axial stress is larger than $0.15F_c$, a more comprehensive interaction formula is used

$$\frac{f_{ca}}{F_c} + \frac{f_{bcx}}{F_{bcx}}.A_1 \leq 1.0 \qquad (2.2)$$

where

$$A_1 = \frac{c_{mx}}{(1 - \frac{f_{ca}}{F_{Ex}})} \qquad (2.3)$$

where A_1 is an amplification factor by which the bending stress is multiplied to account for the destabilizing effect of axial load; c_m is a coefficient that allows for the variable location of the critical section in the length of the

column and sway condition, and F_{Ex} is the Euler stress divided by a factor of safety for buckling. The amplification factor is considered inappropriate for cases where the largest bending stress occurs at one end; the following additional check is required for such cases:

$$\frac{f_{ca}}{0.58F_y} + \frac{f_{bcx}}{F_{bcx}} \leq 1.0 \qquad (2.4)$$

where F_y is the yield stress.

Deflection Criteria

According to the Egyptian specifications, the allowable live load vertical deflection for steel beams with plastered ceilings should not exceed 1/300 of the span, while for the allowable horizontal deflection at the top of a steel building with more than one storey; it should not exceed 1/500 of the total height of the building.

The horizontal deflection at the top of a structure is dependent on factors such as its height-to-width ratio, and its lateral stiffness [1]. In cases where the horizontal deflection at top of structure governs the design, the designer has to be prudent in selecting the elements that are effective in reducing the lateral deflection. The approximate methods that derive the horizontal deflection at the top of several lateral load-resisting systems under the effect of lateral load can be utilized in highlighting the elements that improve the lateral stiffness of several schemes.

Most methods that derive the horizontal deflection at the top of a lateral load-resisting frame are based on the following assumptions: The lateral load is uniformly distributed on the frame; the frame behaves linear elastically, allowing the principle of superposition to be applied; and the sectional properties of all structural elements do not change with height making a closed form solution possible.

Deflection of Rigid Frames

A rigid frame is shown in Fig.(2.1) together with its deflected shape resulting from lateral loading. Rigid frames generally consist of a rectangular grid of horizontal beams and vertical columns connected in the same plane by means of rigid joints. The lateral deflection components of a rigid frame can be thought of as being caused by two components similar to the bending and shear deflection components of a cantilever beam. One component is referred to as the cantilever bending or chord drift component, while the other is referred to as the shear racking component.

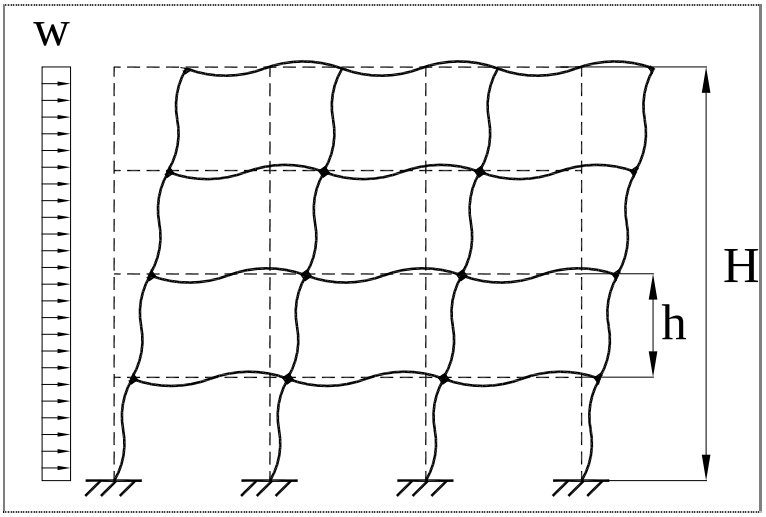

Figure (2.1): Response of rigid frame to lateral loads

Cantilever bending component:

The lateral wind load acting on the vertical face of the frame causes an overturning moment, which reaches its maximum value at the base. In resisting this moment, the frame behaves as a vertical cantilever responding to bending through the axial deformation of columns. The columns lengthen on the windward face of the frame and shorten on the leeward face. This column length change causes the frame to rotate and results in the chord drift component of the lateral deflection. In the case of rigid frames, this mode of deformation accounts for about 20% of the total drift of the frame, and the remaining results from the frame racking [1].

Shear racking component:

The lateral load acting on the rigid frame causes horizontal and vertical shear forces acting on columns and girders respectively, which in turn causes the rotation of joints and bending of members of the frame. In normal proportioned rigid frame, the girder rotation contributes about 65% of the total lateral deflection. The column rotation, on the other hand, contributes about 15% of the lateral drift. This is because in most rigid frames the ratio between column stiffness to girder stiffness is very high, resulting in larger joint rotations. So generally when it is desired to reduce the deflection of rigid frames, we start with girders for adding stiffness [1].

Calculation of drift:

The formula for horizontal deflection at the top of a rigid frame which represents the two modes of deformation is

$$y_{top(rigid-frame)} = \frac{wH^4}{8EI_t} + \left[\frac{Vh^2}{12}\left\{\frac{h}{(\sum EI)_{col}} + \frac{1}{[\sum(EI/L)]_{beam}}\right\}\right].N \qquad (2.5)$$

where w is the uniformly distributed lateral load; H is the total height of the frame; V is the average cumulative shear value per floor; h is the identical story height; N is the number of floors, and EI_t is an expression for the bending stiffness of the rigid frame which increases by increasing the cross sectional area of columns [1].

Deflection of Braced Frames

A braced frame is shown in Fig.(2.2) together with its deflected shape resulting from lateral loading. A braced frame attempts to improve upon the efficiency of pure rigid frame action by virtually eliminating the column and girder bending factors. This is achieved by adding truss members such as diagonals between the floor systems. The shear is now absorbed by the diagonals and not by the girders. The diagonal carry the lateral forces directly in predominantly axial action, providing for nearly pure cantilever action.

The deflection characteristics of a braced frame are similar to those of a cantilever beam. Near the bottom the vertical truss is very stiff, and therefore the floor-to-floor deflections will be less than half the values near the top. Near the top the floor-to-floor deflections increase rapidly mainly due to the cumulative effect of chord drift. The column strains at the bottom of the frame produce a deflection at the top, and since this same effect occurs at every floor, the resulting drift at the top is cumulative. The chord drift problem encountered in practice is very difficult to control and normally requires structural steel quantities well in excess of those required for gravity needs.

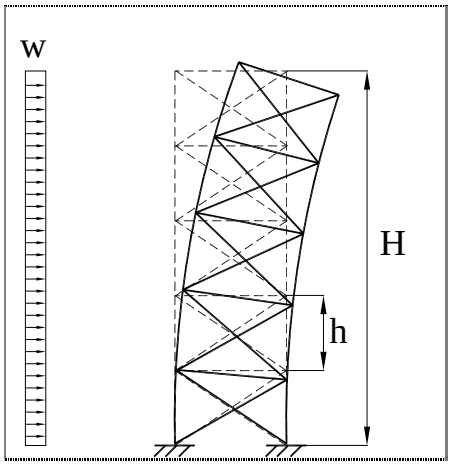

Figure (2.2): Response of braced frame to lateral loads

Calculation of drift:

The formula for horizontal deflection at the top of a braced frame which represents the bending and racking shear deformations is

$$y_{top(braced-frame)} = \frac{wH^4}{8EI_t} + \frac{wH^2}{2GA_t} \qquad (2.6)$$

where *w*, and *H*, have the same meaning as in Eq.(2.5); EI_t is an expression for the bending stiffness of the braced frame which increases by increasing the cross-sectional area of the braced frame columns, and GA_t is an expression for the total racking shear stiffness of braced frame which increases by increasing the cross-sectional area of the X-bracings [5].

Deflection of Braced Frames with Outrigger Trusses

A braced frame with outriggers is shown in Fig.(2.3) together with its deflected shape resulting from lateral loading. The structure comprises a centrally located braced frame with a particular bracing system which is connected to two equal-length outriggers. The outriggers are considered as storey height trusses. The assumed in-plane rigidity of the floor structures will cause identical rotations in the braced frame and façade columns at outrigger level. It is taken that the riggers are attached to the braced frame and exterior columns only, thereby allowing double curvature in the outriggers to take place. The forced double curvature will increase its flexural stiffness.

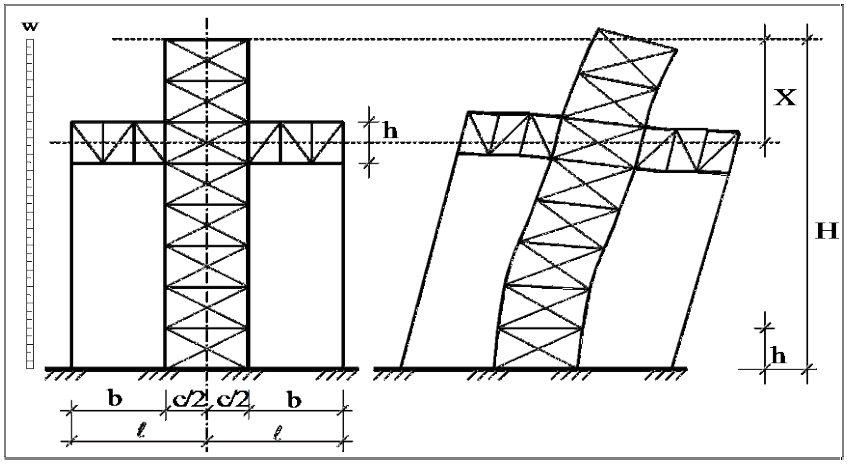

Figure (2.3): Response of braced frame with outrigger to lateral loads

Calculation of drift:

The formula for horizontal deflection at the top of a braced frame with outriggers is

$$y_{top(braced-frame-with-outrigger)} = \frac{wH^4}{8EI_t} + \frac{wH^2}{2GA_t} - \frac{Mr\left(H^2 - x^2\right)}{2EI_t} - \frac{Mr}{\alpha GA_t} \qquad (2.7)$$

where w, and H, have the same meaning as in Eq.(2.5); EI_t and GA_t are the bending and racking shear stiffness respectively of the braced frame; x is the distance measured from the top to the mid height of outrigger; α is a dimensionless parameter equals to *(l/b)* which are clarified in Fig.(2.3), and M_r is the restraining moment [5].

In Eq.(2.7) the first two terms represent the 'free' horizontal deflections of the braced frame at the top due to bending and racking shear as a direct result of lateral loading. The third term is a combination of lateral deflection at outrigger level caused by reverse bending due to M_r and the additional deflection above the outrigger due to rotation at outrigger level. The last term represents a horizontal deflection in the braced frame over a single-storey height at outrigger level.

The only unknown in Eq.(2.7) is the restraining moment M_r, which is developed from a compatibility equation for the rotation at the intersection of neutral lines of the vertical braced frame and the horizontal outrigger. The obtained expression for the restraining moment is

$$M_r = \left\{ \frac{w\left(H^3 - x^3\right)}{6EI_t} + \frac{wx}{\alpha GA_t} \right\} \left\{ \frac{(H-x)}{EI_t} + \frac{1}{h\alpha^2 GA_t} + \frac{b}{24\alpha^2 EI_o} + \frac{1}{h\alpha^2 GA_o} + \frac{(H-x)}{EI_c} \right\}^{-1} \quad (2.8)$$

where w, H, x, α, EI_t and GA_t have the same meaning as in Eq.(2.7); h is the story height at outrigger level; EI_o is an expression for the bending stiffness of the outrigger which increases by increasing the cross-sectional area of the top and bottom chords of the rigger; GA_o is an expression for the total racking shear stiffness of the two outriggers which increases by increasing the cross-sectional area of the bracing of the outrigger, and EI_c is an expression for an overall bending stiffness of the exterior columns which increases by increasing the cross-sectional area of the exterior columns [5].

Concluding remarks:

It is interesting to find out that the deflection reduction of the braced frame is represented in the last two terms in Eq.(2.7), and it is significantly influenced by the location of outrigger. The reduction can be maximized by differentiating Eq.(2.7) with respect to x, setting it equal to zero, and solving for the optimum location of outrigger.

2.3 NEURAL NETWORK LITERATURE REVIEW

2.3.1 Introduction to Neural Networks

The brain's powerful thinking, remembering, and problem solving capabilities have inspired many scientists to attempt computer modeling of its operations. Artificial neural networks (ANNs) are a type of information processing systems, modeled to simulate the biological processes of the brain. Neural networks are so named for their similarity to the way the human brains process information.

2.3.2 Biological Neural System

The brain consists of tens of billions of neurons which are densely interconnected**.** Each neuron is a micro-processing unit built up of three parts: the cell body, the dendrites, and the axon as shown in Fig.(2.4). The axon splits up and connects to dendrites of other neurons through a junction referred to as a synapse. A neuron receives and combines signals from other neurons through dendrites. If combined signal is strong enough, it causes the neuron to fire, producing an output signal. The output signal travels along the axons to other receiving neurons.

The function of the neuron is to integrate the input it receives through its synapses on its dendrites and either generates an action potential or not [6].

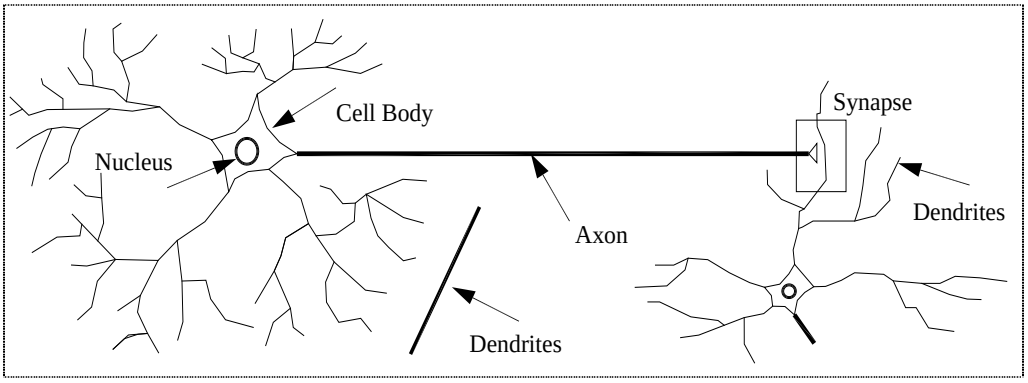

Figure (2.4): Biological Neural System

2.3.3 Neural Computation and Conventional Computation

Neural computing is a rapidly expanding branch of computing concerned with the theory and application of neural networks. Its origins date back to the early 1940s. It has been largely overshadowed since the 1960s by conventional computing, but experienced an upsurge in popularity in the late 1980s as a result of new developments in the field and general advances in computer hardware technology.

The difference between conventional computing and neural computing is in their operating manner. Conventional computing is founded on underlying principles of logic and mathematics. The architecture used by most conventional computers comprises a single central processing unit connected to an area of memory. The memory contains a stored program which is executed in a sequential manner by the processor. Neural computing has another alternative approach, their architecture is like the human brain, consists of a large number of heavily interconnected processing elements which operate in parallel.

2.3.4 Neural Networks

Neural networks are composed of simple elements operating in parallel. As in nature, the network function is determined largely by the connections between elements. We can train a neural network to perform a particular function by adjusting the values of the connections (weights) between elements. Commonly neural networks are adjusted, or trained, so that a particular input leads to a specific target output. Such a situation is shown in Fig.(2.5).

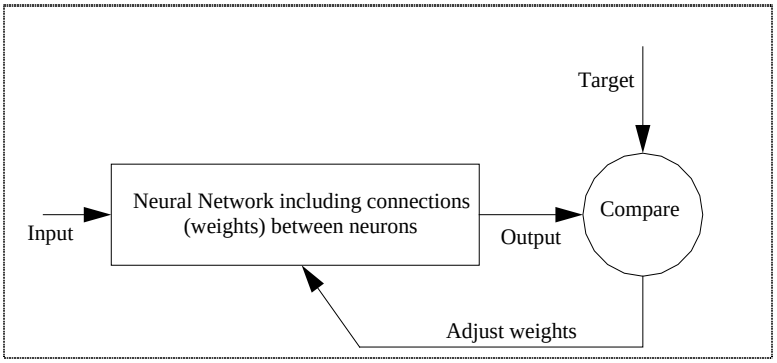

Figure (2.5): Supervised Training Network

The network is adjusted, based on a comparison of the output and the target, until the network output matches the target. Once the weights have been set, the network is able to produce answers for inputs which were not included in the training data [3].

Neural networks have been trained to perform complex functions in various fields of application including pattern recognition, identification, classification, speech, vision, and control systems. Today neural networks can be trained to solve problems that are difficult for conventional computers or human beings.

2.3.5 Neuron Model

2.3.5.1 Single Neuron

A neuron with a single scalar input and no bias is shown on Fig.(2.6a). The scalar input ***P*** is transmitted through a connection that multiplies its strength by the scalar weight ***W***, to form the scalar product ***Wp***. Here the weighted input ***Wp*** is the only argument of the transfer function ***f***, which produces the scalar output ***a***.

The scalar bias ***b*** can be considered as an additional input to the transfer function ***f***, as shown on Fig.(2.6b). It is presented as simply being added to the product ***Wp*** by the summing junction or as shifting the function ***f*** to the left by an amount ***b***. The bias is much like a weight, except that it has a constant input of one. Both ***W***, and ***b*** are adjustable scalar parameters for the neuron.

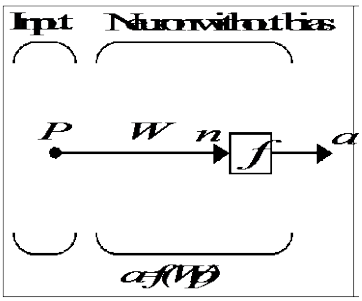

Figure (2.6a) Single neuron without bias

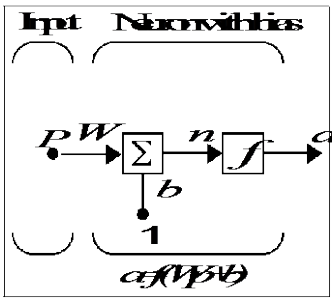

Figure (2.6b) Single neuron with bias

The transfer function ***f*** is a step function or a sigmoid function, which takes the argument ***n*** and produces the output ***a***. The selection of the transfer function is decided based on the neural network learning technique.

2.3.5.2 Neuron with Vector Input

A neuron with a single R-element input vector is shown on Fig.(2.7). Here the individual element inputs (P_1, P_2,... P_R), are multiplied by weights ($W_{1,1}$, $W_{1,2}$, ... $W_{1,R}$), and the weighted values are fed to the summing junction. Their sum is simply ***Wp***, the dot product of the (single row) matrix ***W*** and the vector ***P***.

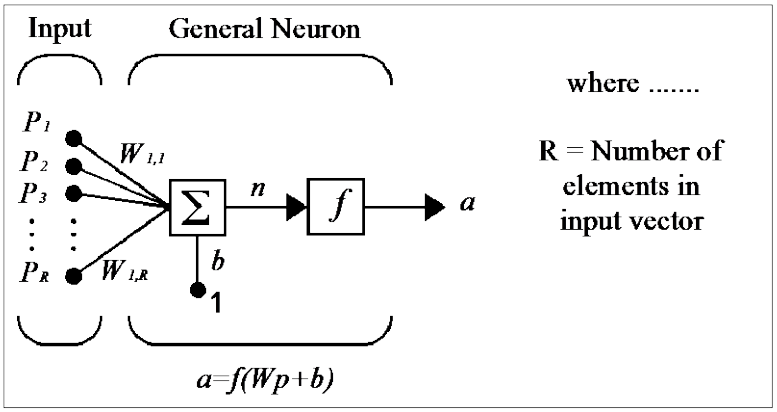

Figure (2.7): Neuron with Vector Input

The neuron has a bias ***b***, which is summed with the weighted inputs to form the net input ***n***. This sum ***n***, is the argument of the transfer function ***f***.

$$n = W_{1,1}.P_1 + W_{1,2}.P_2 + ... + W_{1,R}.P_R + b$$

2.3.6 Network Architectures

The art of using neural networks revolve around the myriad of ways the individual neurons can be clustered together. This clustering occurs in the human mind in such a way that information can be processed in a dynamic, interactive and self-organizing way. Biologically, neural networks are constructed in a three-dimensional world from microscopic components.

Currently, neural networks are the simple clustering of the primitive artificial neurons. This clustering occurs by creating layers which are then connected to one another. How these layers connect is the art of engineering networks to resolve real world problems.

Basically, all artificial neural networks have a similar structure or topology as shown in Fig.(2.8). In that structure some of the neurons interface to the real world to receive its inputs. Other neurons provide the real world with the network's outputs. All the rest of the neurons are hidden from view.

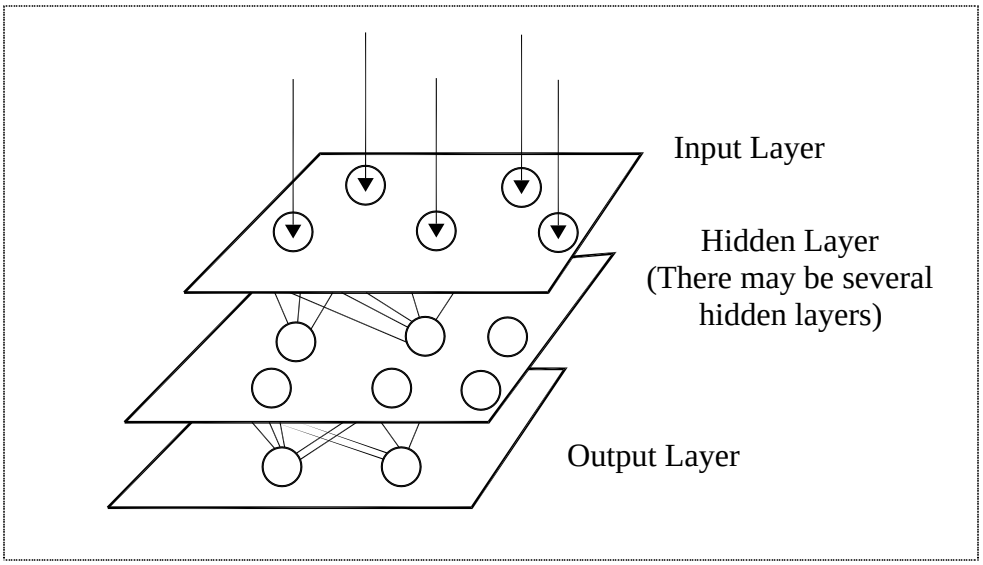

Figure (2.8): Simple Neural Network Diagram

2.3.6.1 Layer of Neurons

A one-layer network with ***R*** input elements and **S** neuron is shown on Fig.(2.9a). In this network, each element of the input vector ***P*** is connected to each neuron input through the weight matrix ***W***. The *i*th neuron has a summer that gathers its weighted inputs and bias to form its own scalar output *n(i)*. The various *n(i)* taken together form an *S*-element net input vector ***n***. Finally, the neuron layer outputs form a column vector ***a***. The ***S*** neuron ***R*** input one-layer network also can be drawn in abbreviated notation as shown on Fig. (2.9b).

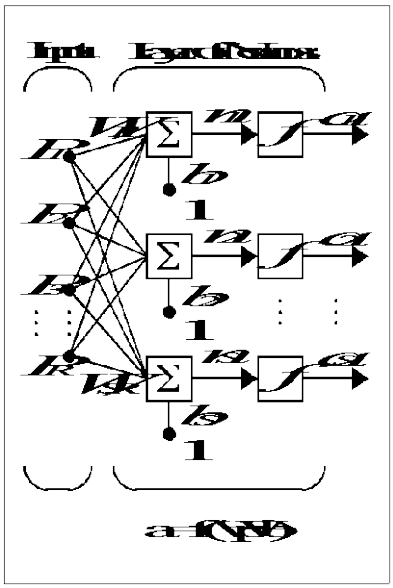

Figure (2.9a) Detailed one-layer Network

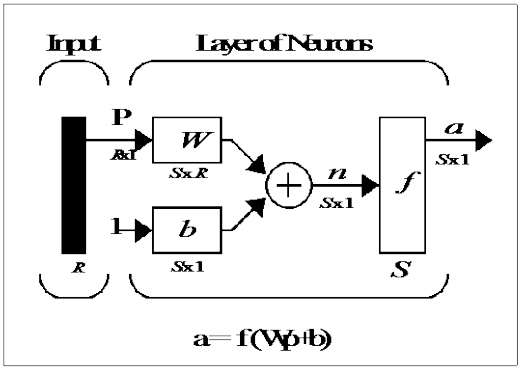

Figure (2.9b) Abbreviated one-layer Network

2.3.6.2 Multiple Layers of Neurons

A network can have several layers. Each layer has a weight matrix ***W***, a bias vector **b**, and an output vector **a**. The network shown on Fig.(2.10) has ***R*** inputs, ***S1*** neurons in the first layer, ***S2*** neurons in the second layer, etc. It is common for different layers to have different numbers of neurons. For each neuron there is a constant input one is fed to the biases. The network also has an input weight (**IW**) matrix connected to the input vector ***P***, and other layer weight (**LW**) matrices.

The outputs of each intermediate layer are the inputs to the following layer. Thus layer 2 can be analyzed as a one-layer network with ***S1*** inputs, ***S2*** neurons, and an *S*2x*S*1 weight matrix ***W2***. The input to layer 2 is ***a1***; the output is ***a2***. This approach can be taken with any layer of the network. The layers of a multilayer network play different roles. The layer that receives network inputs is called an *input layer*, the layer that produces the network output is called an *output layer*, and all the other layers are called *hidden layers*.

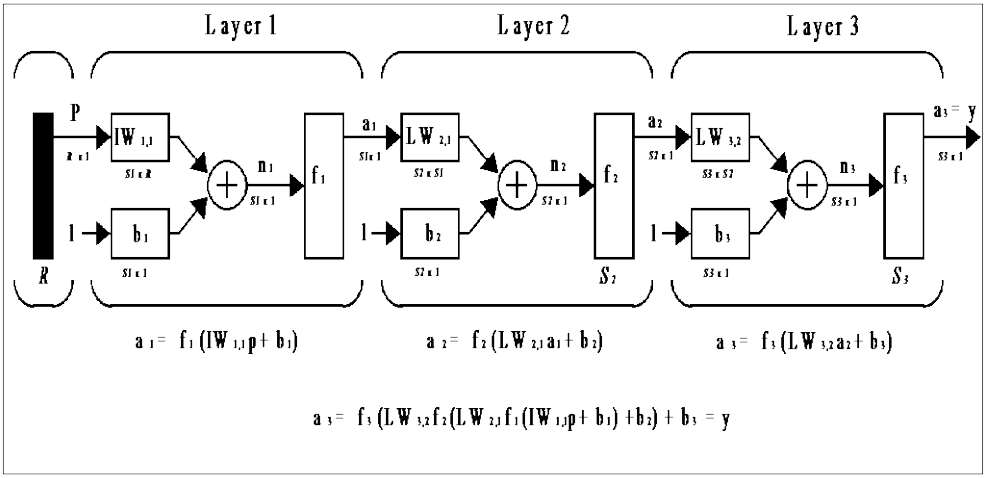

Figure (2.10): Multiple layer Network

2.3.6.3 Feed-Forward Architecture

Feed-forward ANNs allow signals to travel one way only; from input to output. There is no feedback (loops) i.e. the output of any layer does not affect that same layer. Feed-forward ANNs tend to be straight forward networks that associate inputs with outputs. They are extensively used in pattern recognition and function approximation applications [3].

2.3.6.4 Feedback Architecture

Feedback networks can have signals traveling in both directions by introducing loops in the network. Feedback networks are very powerful and can get extremely complicated. Feedback networks are dynamic; their state is changing continuously until they reach an equilibrium point. They remain at the equilibrium point until the input changes and a new equilibrium needs to be found. Feedback architectures are also referred to as interactive or recurrent, although the latter term is often used to denote feedback connections in single-layer organizations.

2.3.7 The learning Process

Every neural network possesses knowledge which is contained in the values of the weights. The process of modifying the knowledge stored in the network is known by the learning process. This process requires a learning rule or what

we refer to as a training algorithm. The learning rule is defined as a procedure for modifying the weights and biases of a network. Learning rules fall into two broad categories: supervised learning, and unsupervised learning.

In ***supervised learning***, the learning rule is provided with a set of examples (*the training set*). As the inputs are applied to the network, the network outputs are compared to the targets. The learning rule is then used to adjust the weights and biases of the network in order to move the network outputs closer to the targets.

In ***unsupervised learning***, the weights and biases are modified in response to network inputs only. There are no target outputs available. Most of these algorithms perform clustering operations. They categorize the input patterns into a finite number of classes. This is useful in some applications such as vector quantization.

2.3.8 Training

The training process requires a set of examples of proper network behavior (network inputs "***P***" and target outputs "***t***"). During training the weights and biases of the network are iteratively adjusted to minimize the network performance function. This function can be described by the mean square error (mse) function which defines the average squared error between the network outputs "***a***" and the target outputs "***t***"**,** or any other specified function.

Several training algorithms use the gradient of the performance function to determine how to adjust the weights to minimize performance. The gradient is determined using a technique called back propagation. This technique involves performing computations backwards through the network, which are derived using the chain rule of calculus.

2.3.9 Limitations and Cautions

To develop a proper model design for a neural network, we should consider the following limitations and cautions:

- It is undesirable to train large networks with few training pairs. This will produce underdetermined neural networks, in which the number of training pairs are fewer than the number of underdetermined parameters (weights and biases) associated with the network. Such networks when trained will yield different approximations [7].

- It is undesirable to use input vector whose length is much larger or smaller than the other input vectors. An input vector with large elements can lead to changes in the weights and biases that take a long time for a much smaller input vector to overcome. Before training, it is often useful to scale the inputs and targets so that they always fall within a specified range. The normalized inputs and targets will decrease training time [3].

- It is not preferable to produce a powerful network -with high number of neurons, iteration trials (epochs), and hidden layers – without checking its ability to generalize, as one of the problems that occurs during neural network training is known by over fitting. The error on the training set is driven to a very small value, but when new data is presented to the network the error is large. In this case the network has memorized the training examples, but it has not learned to generalize to new situations [3].

- It is essential to reinitialize the network and retrain it several times to guarantee the approach to an optimal solution. Although a multilayer backpropagation network with enough neurons can implement just about any function, but it will not always find the correct weights for the best solution. The reason for this is that the error surface of a nonlinear network is more complex than the error surface of a linear network. To understand this complexity see Figs.(2.11a) and (2.11b), which show two different error surfaces for a multilayer network. The problem is that nonlinear transfer functions in multilayer networks introduce many local minima in the error surface. As gradient descent

is performed on the error surface it is possible for the network solution to become trapped in one of these local minima. This may happen depending on the initial starting conditions. Settling in a local minimum may be good or bad depending on how close the local minimum is to the global minimum and how low an error is required.

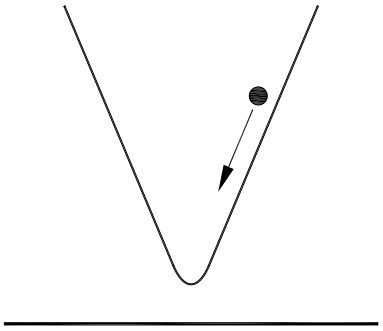

Figure (2.11a): Simple Error Surface

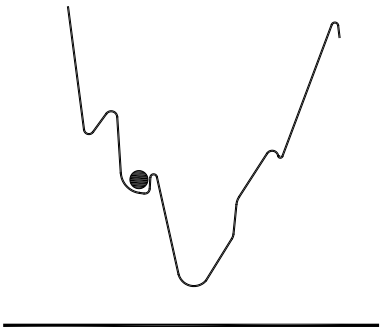

Figure (2.11b): Complex Error Surface

2.3.10 Neural Networks Applications

Within the last several years, researches have begun to investigate the potential of artificial neural networks (ANNs) as a tool for supporting the modeling of engineering systems. ANNs have been applied in many fields as in aerospace (in aircraft control systems, autopilot enhancements, aircraft component simulation, aircraft component fault detection), defense (in weapon steering, target tracking, object discrimination, facial recognition, sonar, radar and image signal processing including feature extraction and noise suppression, signal/image identification), electronics (in process control, machine vision, voice synthesis, nonlinear modeling), financial (in real estate appraisal, loan advisor, corporate bond rating, credit-line use analysis, portfolio trading program, corporate financial analysis, currency price prediction), industrial (in predicting the output gasses of furnaces and other industrial processes), manufacturing (in product design and analysis, process and machine diagnosis, visual quality inspection systems, welding quality analysis, paper quality prediction, machine maintenance analysis, project

bidding, planning and management, dynamic modeling of chemical process system), and telecommunication (in image and data compression, automated information services, real-time translation of spoken language, customer payment processing systems).

From the presented applications, it is clear that neural networks may play a role in addressing the tasks of, interpretation, prediction, modeling, classification, identification and estimation.

2.3.10.1 Neural Networks in Civil Engineering

Neural networks applications in civil engineering only go back to the late 1980s , but already cover a range of topics as prediction of river flow [8], design of coastal sewage systems [9], computing truck attributes (such as velocity, axle spacing, and axle loads) [10], stress strain modeling of soil [11], prediction of pile capacity [12], identification of natural modes[13], structural damage detection [14], decentralized control of cable-stayed bridge [15], prediction of cost for buildings [16], estimating the productivity of concreting activities [17], and exploring concrete slump model [18].

2.3.10.2 Neural Networks in Structural Engineering

Neural networks have also been used widely in structural engineering applications, as in estimation of seismic response of buildings [19], prediction of buckling load of columns [20], optimization of cold-formed steel beams [21], modeling the capacity of pin-ended slender reinforced concrete columns [22], determining the shear strength of reinforced concrete deep beams [23], and classifying steel semi-rigid connections [24].

CHAPTER (3)

TOOLS AND ANALYSIS

3.1 OBJECTIVE

An important task is to derive the relation between the lateral load-resisting systems for multi-story steel frames and their expected lateral drift and optimum weight in order to prepare the input data for training and testing the artificial neural network. In this chapter, the design procedures for the three different types of lateral load-resisting frames are briefly explained.

To perform the analysis, it is necessary to define the considered frames configurations and design loads, choose suitable cross-section profiles, and check steel design strength and serviceability. In this section, the assumptions upon which the analysis is based are presented.

The analysis in this task is performed using a finite-element program, and the design is implemented using a set of auxiliary programs specially developed to achieve the optimal design of sections. Design procedures and tools are described in this section.

3.2 ASSUMPTIONS

3.2.1 Frames Configurations

The analysis addresses rigid frames, braced frames, and braced frames with single outrigger truss.

The frames have constant bay width, height and spacing of 4.0 meters. The studied frames are subdivided into 4 groups which are 3-bay group with 12m wide, 4-bay group with 16m wide, 5-bay group with 20m wide and 6-bay group with 24m wide. The considered heights are 20, 40, 60, 80, 100, 120, 140, 152, 160 meters.

The braced frames considered all possible cases for braced bays. The braced frames with outrigger truss are analyzed with only one braced bay, except for the 6-bay group it is analyzed using also two braced bays.

Figures (3.1) to (3.4) present samples of the studied frame configurations of the 3-bay, 4-bay, 5-bay, and 6-bay groups, respectively.

Generally in the presented illustrations rigid frames are denoted as “Rigid”, braced frames are denoted as “Br. (number of braced bays ‘B’)”, and braced frames with single outrigger truss are denoted as “OR. (number of braced bays ‘B’)”.

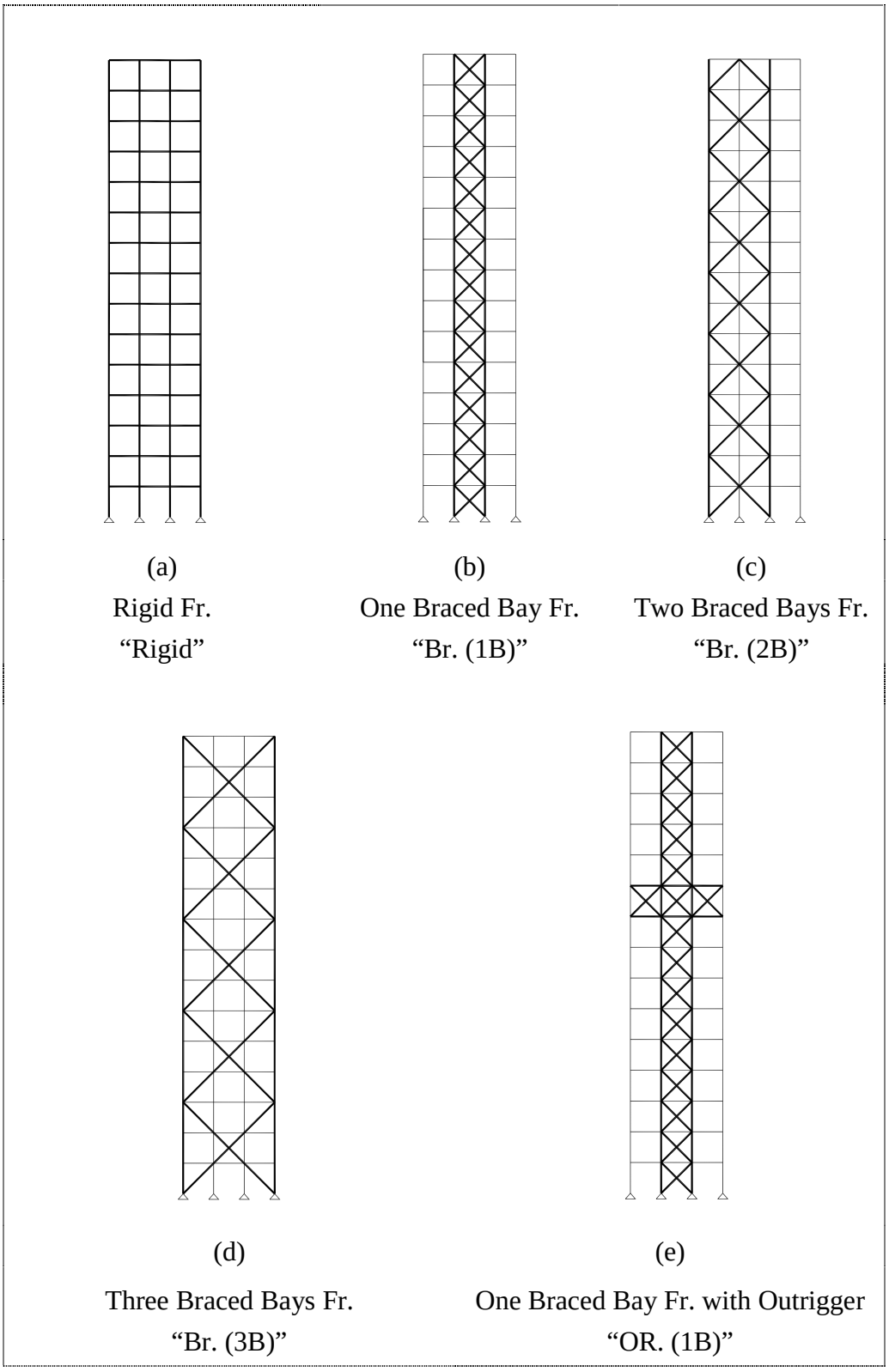

Figure (3.1): Lateral Load-resisting Frames for 3-Bay Group with 15 Stories

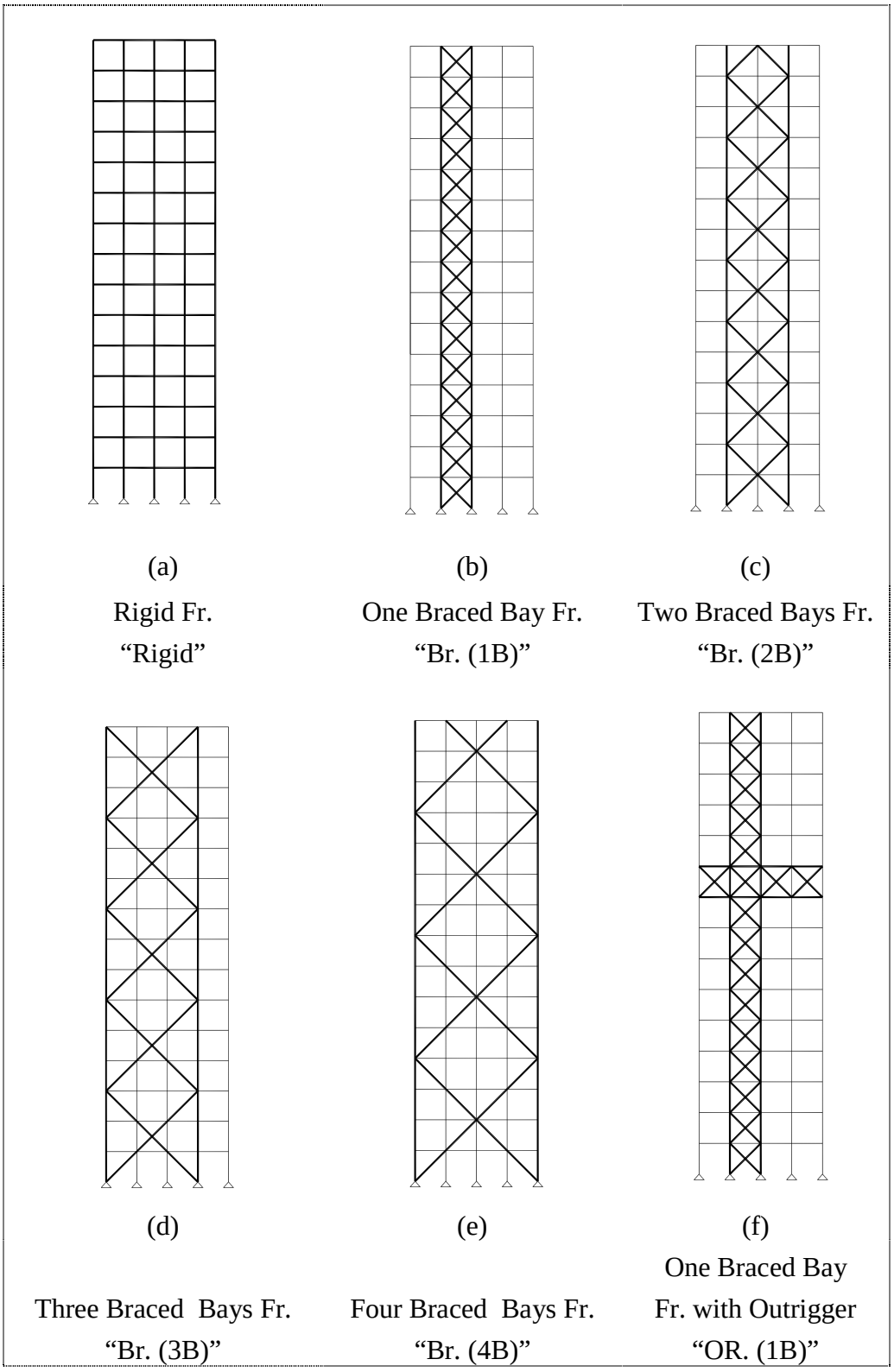

Figure (3.2): Lateral Load-resisting Frames for 4-Bay Group with 15 Stories

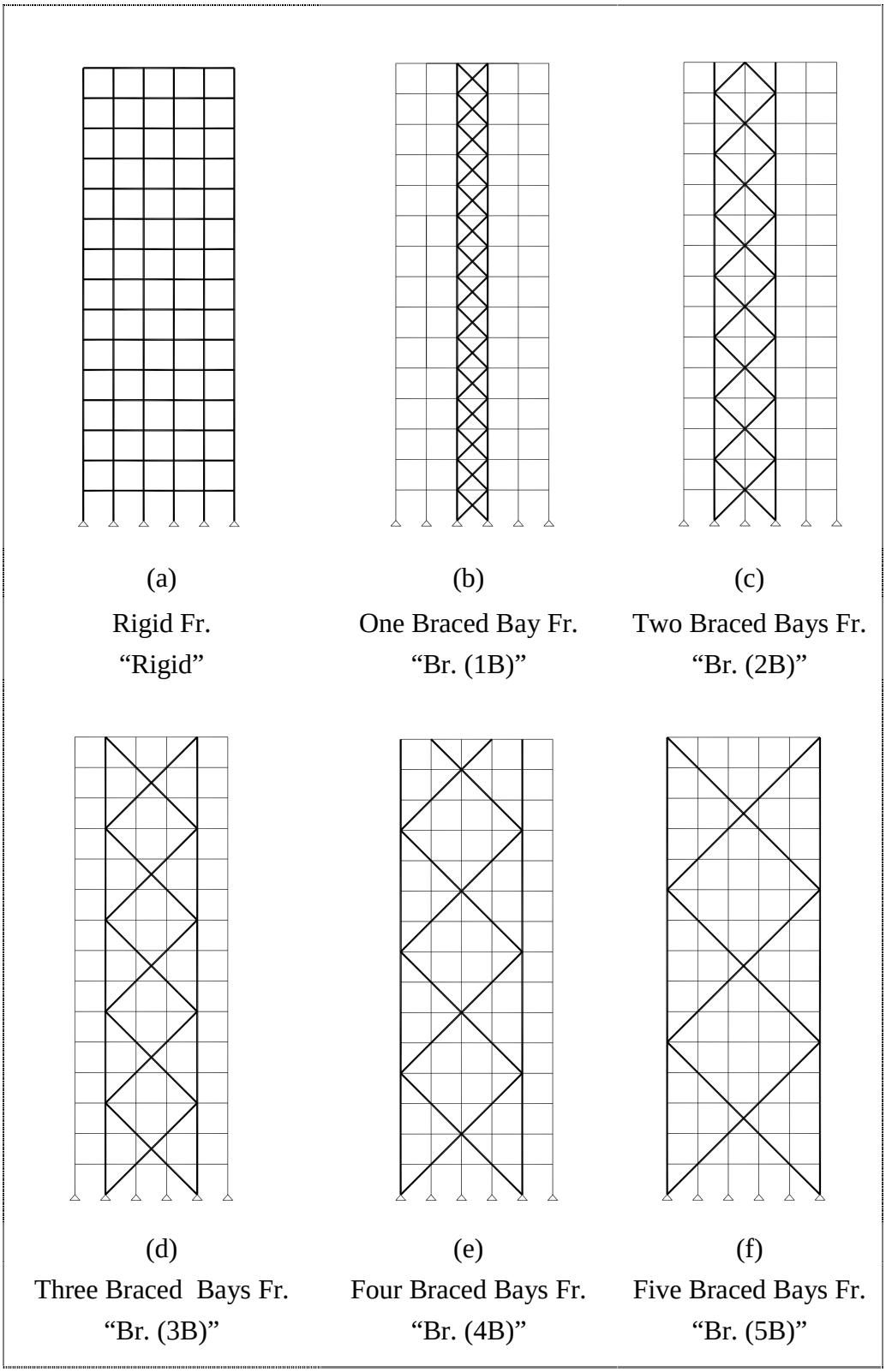

Figure (3.3): Lateral Load-resisting Frames for 5-Bay Group with 15 Stories

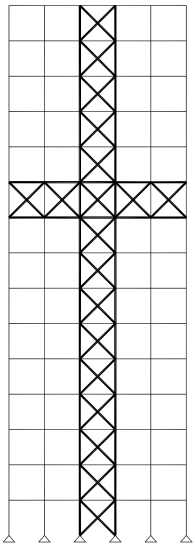

(g)
One Braced Bay Fr. with Outrigger
"OR. (1B)"

Figure (3.3) cont.: Lateral Load-resisting Frames for 5-Bay Group with 15 Stories

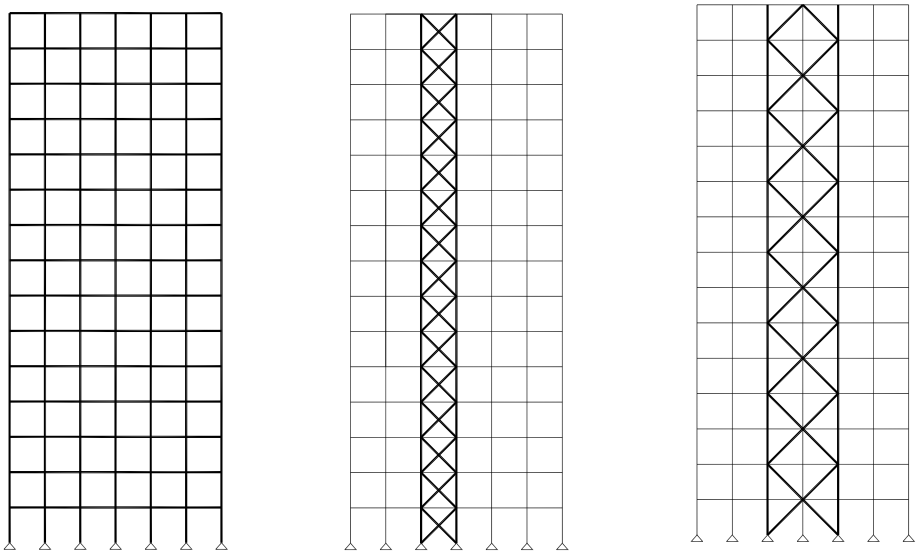

(a)
Rigid Fr.
"Rigid"

(b)
One Braced Bay Fr.
"Br. (1B)"

(c)
Two Braced Bays Fr.
"Br. (2B)"

Figure (3.4): Lateral Load-resisting Frames for 6-Bay Group with 15 Stories

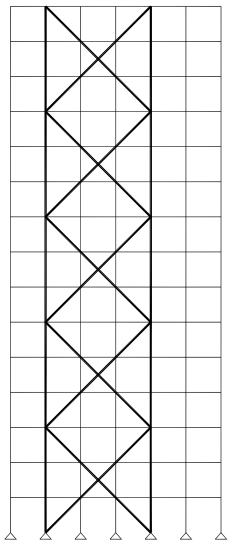

(d)
Three Braced Bays Fr.
"Br. (3B)"

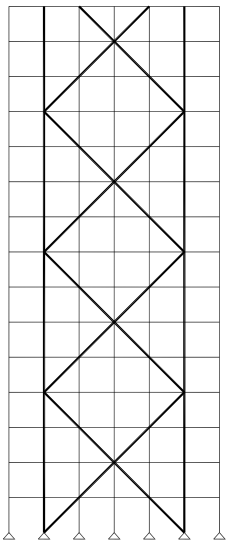

(e)
Four Braced Bays Fr.
"Br. (4B)"

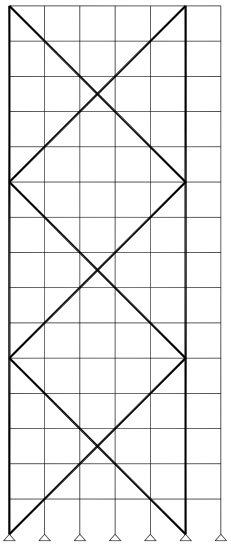

(f)
Five Braced Bays Fr.
"Br. (5B)"

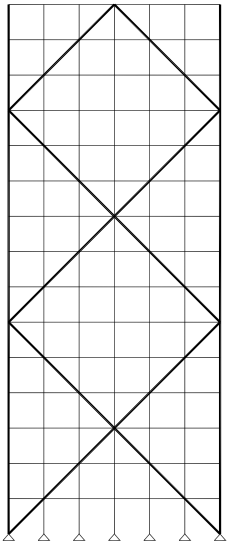

(g)
Six Braced Bays Fr.
"Br. (6B)"

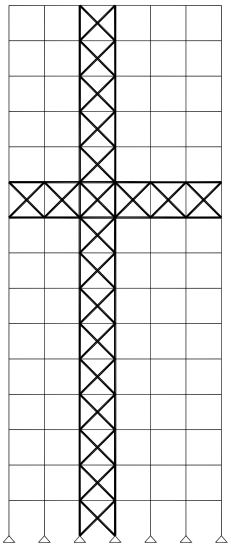

(h)
One Braced Bay Fr.
with Outrigger
"OR. (1B)"

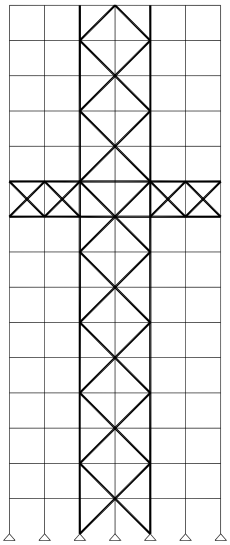

(k)
Two Braced Bay Fr.
with Outrigger
"OR. (2B)"

Figure (3.4) cont.: Lateral Load-resisting Frames for 6-Bay Group with 15 Stories

3.2.2 Section Profiles

Steel profiles used for sizing girders and columns of the analyzed frames are standard hot rolled wide-flange shapes possessing an axis of symmetry about the plane of bending, whereas for the bracing members circular hollow sections are used. To simplify the selection of profiles, standard rolled section tables are utilized in the design.

For girders sizing, it is necessary to consider that rigid frames girders require heavier profiles than those required for braced frames girders. The standard HEA rolled steel sections are used for rigid frame girders limited to HEA600, and the standard IPE sections are used for braced frame girders.

For columns sizing, the standard HEB rolled sections are used. In cases where the design requirements exceeded the largest available HEB section, welded cover plates are added to the flanges of the rolled section as shown in Fig.(3.5). The maximum plate's width and thickness are 500 and 50 millimeters, respectively.

Bracing elements are sized with the standard pipes limited to 66.0 cm diameter.

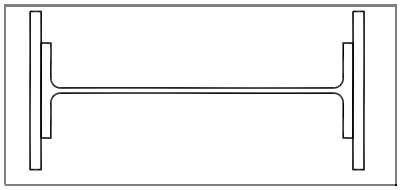

Figure (3.5): HEB 1000 with welded cover plates

3.2.3 Design Considerations

Specifications:

The design is to conform with the Egyptian Code of Practice for Steel Constructions and Bridges [4] using high grade steel ST-52 with yield strength 3.60 t/cm^2 for thicknesses less than or equal to 40 mm, and 3.35 t/cm^2 for thicknesses greater than 40 mm. The maximum lateral drift is limited to 1/500 of the frame height.

Loads:

The frames are analyzed under the effect of uniform dead loads of 2.2 t/m', uniform live loads of 1.0 t/m', and lateral wind loads distributed according to Egyptian Specifications for Loads with wind intensity equal to 0.08 t/m^2. The analysis considered the critical load combinations of loads.

Recommendations for Optimum lateral drift:

The location of both the braced bay in braced frames and the outrigger truss in braced frames with outrigger truss have a significant influence on the maximum lateral drift exerted on the frame.

The location of the braced bay in braced frames is preferable to be at centre or close to centre of frame. This will not induce additional lateral drift on frame under vertical load due to unsymmetrical vertical stiffness.

The location of single outrigger truss for optimum lateral drift has been investigated based on J.C.D. Hoenderkamp and M.C.M. Bakker method [5] which has been mentioned in Chapter (2). The optimum location for the outrigger truss is selected after several trials of substitution in Eqs.(2.7) and (2.8) and comparison of results for the studied frames. It is often taken at a distance equal to 1/3 of the total height of frame measured from the top.

Table (3.1) presents the selected locations of the outrigger truss for the studied 4 groups of frames.

Table (3.1): Location of Outrigger Truss.

Frame's total number of stories	40	38	35	30	25	20	15	10	5
The i th story level for outrigger truss	27	26	24	21	17	14	10	7	3

3.2.4 Design Procedures and Tools

Design is an iterative process. The sections used to run the original analysis are not typically the same sections that are chosen at the end of the design process. It is always wanted to ensure that the frame analysis is performed using the final frame section sizes and then a design check is implemented based on the forces obtained from that analysis.

Analysis is performed using SAP2000 [25] software program for the structural analysis and design of structures. The version used is 9.0.3. It allows the import and export of data in an excel spread sheet format, which is very useful in controlling the implementation of the iterative design process as will be described later. In addition to that, it allows for lateral displacement optimization, where it can predict which members should be increased in size to control the displacements based on the energy per unit volume in the members.

Design can not be completely implemented by SAP2000 [25] for two reasons. The first reason is that SAP2000 module design does not support Egyptian specifications. Second reason is that SAP2000 design can not guarantee that sizing of columns will decrease along their height.

Three auxiliary programs are developed for the design of the three different types of lateral load-resisting frames. Running each program individually will start the design verifications for each member in the prescribed frame and returns new sections for the optimum design. The resulting sections will overcome the irregularity problem in sizing columns of frame, and will be organized in a spread sheet format that can be easily imported to the frame model for a new iteration of analysis.

The following is the typical procedures for the design process:

1. Create the frame model taking into consideration that labeling of members has be arranged in a sequential order for the manipulation of importing data to the auxiliary design programs, and exporting the new

sections design to the SAP frame model. Also size the elements with preliminary section profiles.

2. Perform the analysis of the frame model using SAP2000 program.
3. Export the SAP input and output data of the model to an excel file.
4. Perform the design using one of the auxiliary design programs, according to the prescribed frame system.
5. Exchange the current section profiles in the excel SAP input file with the new sections design created by the design program.
6. Repeat steps 3 to 5 and then compare the maximum lateral drift with the constrained value.
7. If the lateral drift is less than the constrained value then continue with the design iterations procedures by repeating steps 3 to 5 until the last used analysis section profiles for the frame elements are identical to the new design section profiles.
8. If the lateral drift is greater than the constrained value then continue the iterations using SAP2000, by adjusting the model for lateral displacement optimization requirements, and activating the lateral displacement target option.

Figure (3.6) presents a diagram for the typical procedures in the design process, starting with the creation of frame model and ending with listing data for the ANN modeling.

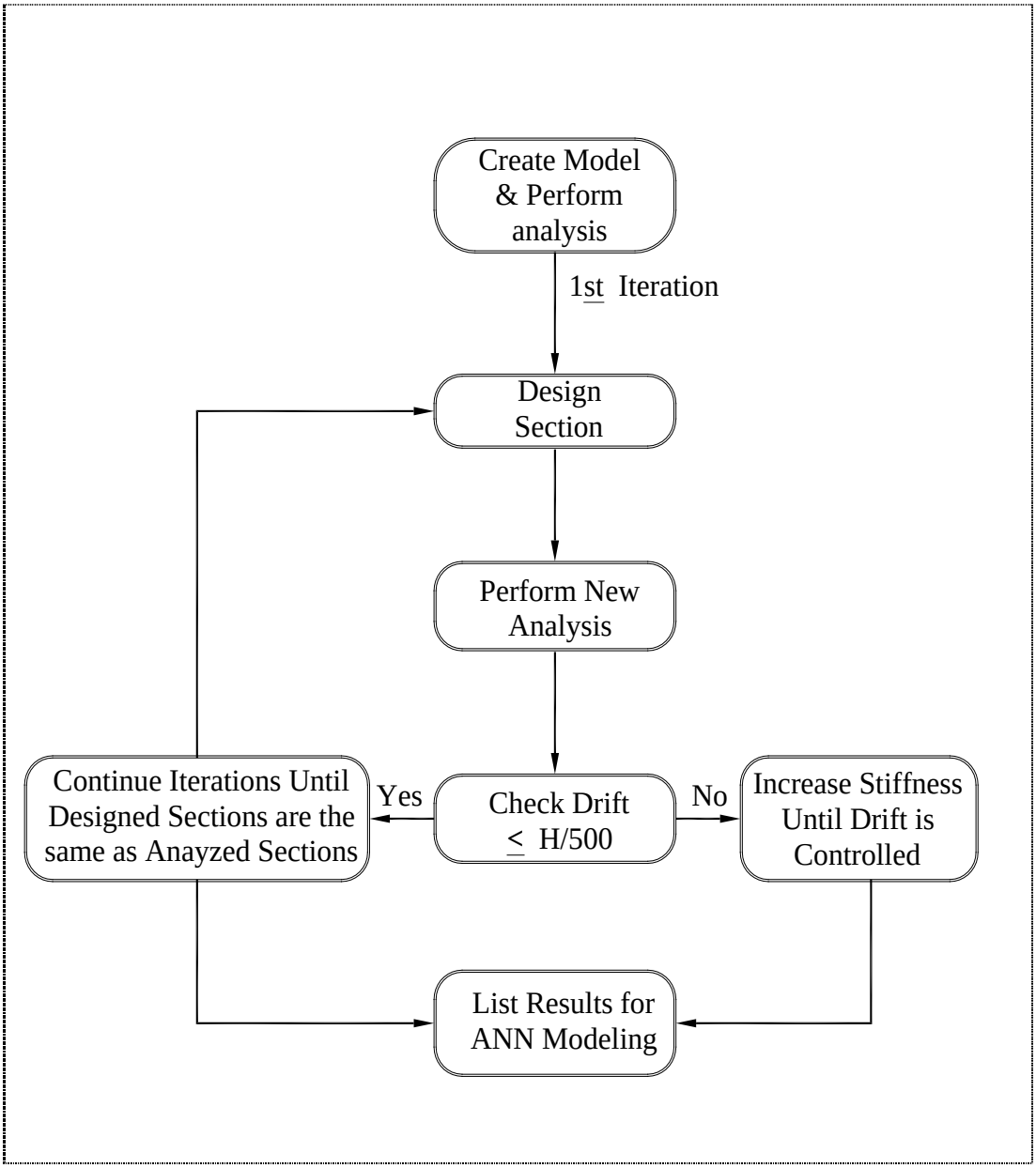

Figure (3.6): Diagram for Design Procedures

Auxiliary programs:

In most frame cases when the strength governs the design, the design process is implemented with a set of auxiliary programs generated with MATLAB language for technical computation [26].

MATLAB is very useful in solving problems that include math calculations and algorithm development. Its basic data element is an array that does not require dimensioning. It is capable to read input data from an excel file and to write output data in an excel file. In the design process, the source of input data to run the generated programs is the sap output files exported with an excel format.

Each lateral load-resisting system has its own design requirements that slightly differ than the others. For example: rigid frames design require the evaluation of buckling coefficient *K* for the columns based on end restraints offered by the girders, also braced frames design require the verification of bracing elements without considering wind load combinations as secondary load case.

To simplify the design process each lateral load-resisting system has its design program as follows: the “RGFDES” program is created for the rigid frames design; “BRFDES” program is created for the braced frames design, and “ORFDES” is created for the braced frames with outrigger truss. The three programs require before operating the identification of SAP output file, and number of stories and bays of the frame. The “BRFDES” and “ORFDES” programs require in addition to that, the identification of number of braced bays.

Figure (3.7) presents the screen of the “BRFDES” program while operating. It shows that the program is supplied with the identification items of 4-bay frame with 20 stories, and four braced bays.

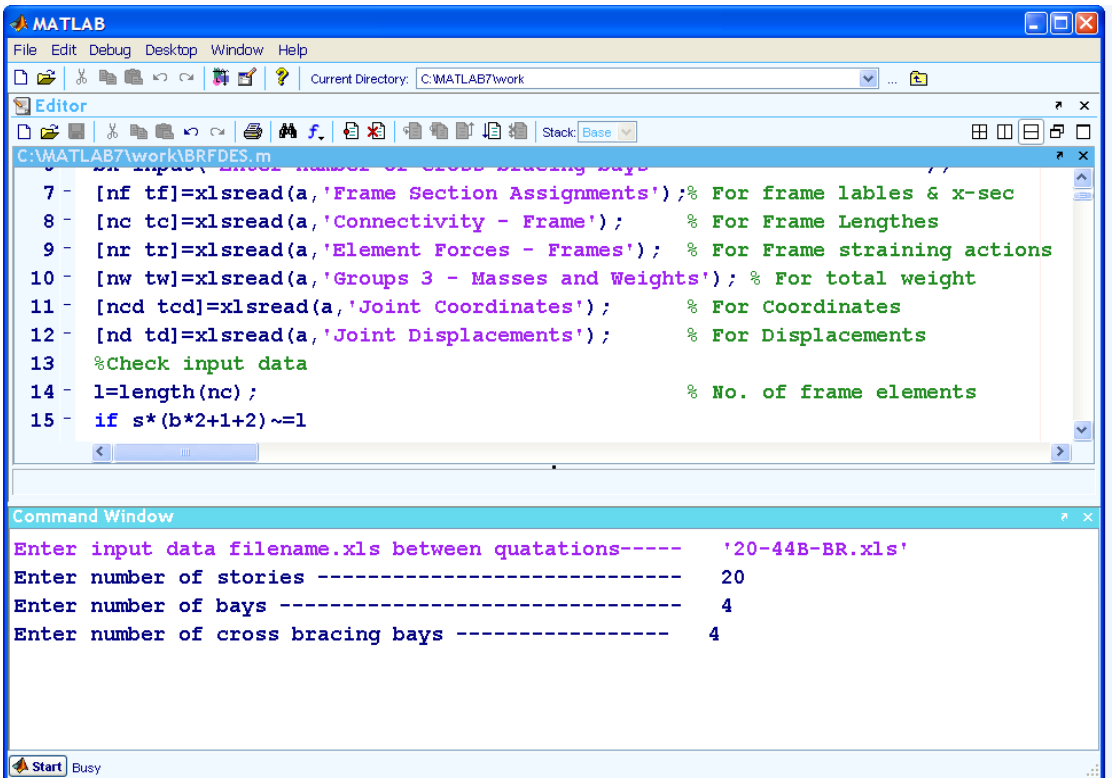

Figure (3.7): “BRFDES” Program while Operating

The output for the three design programs has the same organization. Figure (3.8) presents a screen for a design output excel file created for a 4-bay frame with 20 stories, and four braced bays.

It can be seen that row “3” displays the frame’s total weight followed by the maximum lateral displacement exerted on the frame. Also, column “A” displays the labels of frame elements, followed by columns that display the relevant frame section properties. Column “AO” displays the critical unit of check for the normal stresses interaction formulas which where previously mentioned in clause (2.2.1). Column “AZ” displays the expected optimized sections, and column “AP” displays the expected unit of check for the optimized sections. Finally column “BJ” displays the new sections that will be utilized in the next iteration of analysis after filtering the sizes causing irregularity in columns.

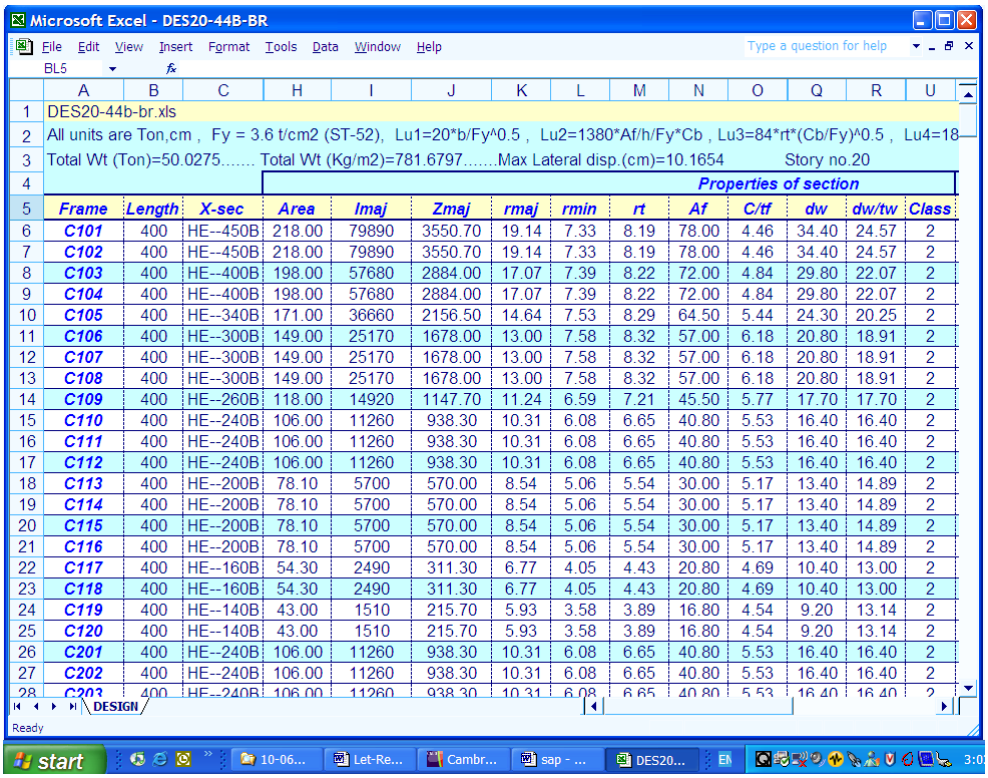

Microsoft Excel - DES20-44B-BR

File Edit View Insert Format Tools Data Window Help — Type a question for help

BL5

DES20-44b-br.xls

All units are Ton,cm , Fy = 3.6 t/cm2 (ST-52), Lu1=20*b/Fy^0.5 , Lu2=1380*Af/h/Fy*Cb , Lu3=84*rt*(Cb/Fy)^0.5 , Lu4=18

Total Wt (Ton)=50.0275..... Total Wt (Kg/m2)=781.6797.....Max Lateral disp.(cm)=10.1654 Story no.20

				Properties of section										
Frame	Length	X-sec	Area	Imaj	Zmaj	rmaj	rmin	rt	Af	C/tf	dw	dw/tw	Class	
C101	400	HE--450B	218.00	79890	3550.70	19.14	7.33	8.19	78.00	4.46	34.40	24.57	2	
C102	400	HE--450B	218.00	79890	3550.70	19.14	7.33	8.19	78.00	4.46	34.40	24.57	2	
C103	400	HE--400B	198.00	57680	2884.00	17.07	7.39	8.22	72.00	4.84	29.80	22.07	2	
C104	400	HE--400B	198.00	57680	2884.00	17.07	7.39	8.22	72.00	4.84	29.80	22.07	2	
C105	400	HE--340B	171.00	36660	2156.50	14.64	7.53	8.29	64.50	5.44	24.30	20.25	2	
C106	400	HE--300B	149.00	25170	1678.00	13.00	7.58	8.32	57.00	6.18	20.80	18.91	2	
C107	400	HE--300B	149.00	25170	1678.00	13.00	7.58	8.32	57.00	6.18	20.80	18.91	2	
C108	400	HE--300B	149.00	25170	1678.00	13.00	7.58	8.32	57.00	6.18	20.80	18.91	2	
C109	400	HE--260B	118.00	14920	1147.70	11.24	6.59	7.21	45.50	5.77	17.70	17.70	2	
C110	400	HE--240B	106.00	11260	938.30	10.31	6.08	6.65	40.80	5.53	16.40	16.40	2	
C111	400	HE--240B	106.00	11260	938.30	10.31	6.08	6.65	40.80	5.53	16.40	16.40	2	
C112	400	HE--240B	106.00	11260	938.30	10.31	6.08	6.65	40.80	5.53	16.40	16.40	2	
C113	400	HE--200B	78.10	5700	570.00	8.54	5.06	5.54	30.00	5.17	13.40	14.89	2	
C114	400	HE--200B	78.10	5700	570.00	8.54	5.06	5.54	30.00	5.17	13.40	14.89	2	
C115	400	HE--200B	78.10	5700	570.00	8.54	5.06	5.54	30.00	5.17	13.40	14.89	2	
C116	400	HE--200B	78.10	5700	570.00	8.54	5.06	5.54	30.00	5.17	13.40	14.89	2	
C117	400	HE--160B	54.30	2490	311.30	6.77	4.05	4.43	20.80	4.69	10.40	13.00	2	
C118	400	HE--160B	54.30	2490	311.30	6.77	4.05	4.43	20.80	4.69	10.40	13.00	2	
C119	400	HE--140B	43.00	1510	215.70	5.93	3.58	3.89	16.80	4.54	9.20	13.14	2	
C120	400	HE--140B	43.00	1510	215.70	5.93	3.58	3.89	16.80	4.54	9.20	13.14	2	
C201	400	HE--240B	106.00	11260	938.30	10.31	6.08	6.65	40.80	5.53	16.40	16.40	2	
C202	400	HE--240B	106.00	11260	938.30	10.31	6.08	6.65	40.80	5.53	16.40	16.40	2	
C203	400	HE--240B	106.00	11260	938.30	10.31	6.08	6.65	40.80	5.53	16.40	16.40	2	

DESIGN

Ready

start 10-06... Let-Re... Cambr... sap - ... DES20... EN 3:0

Figure (3.8): Sample of Design Output Excel File

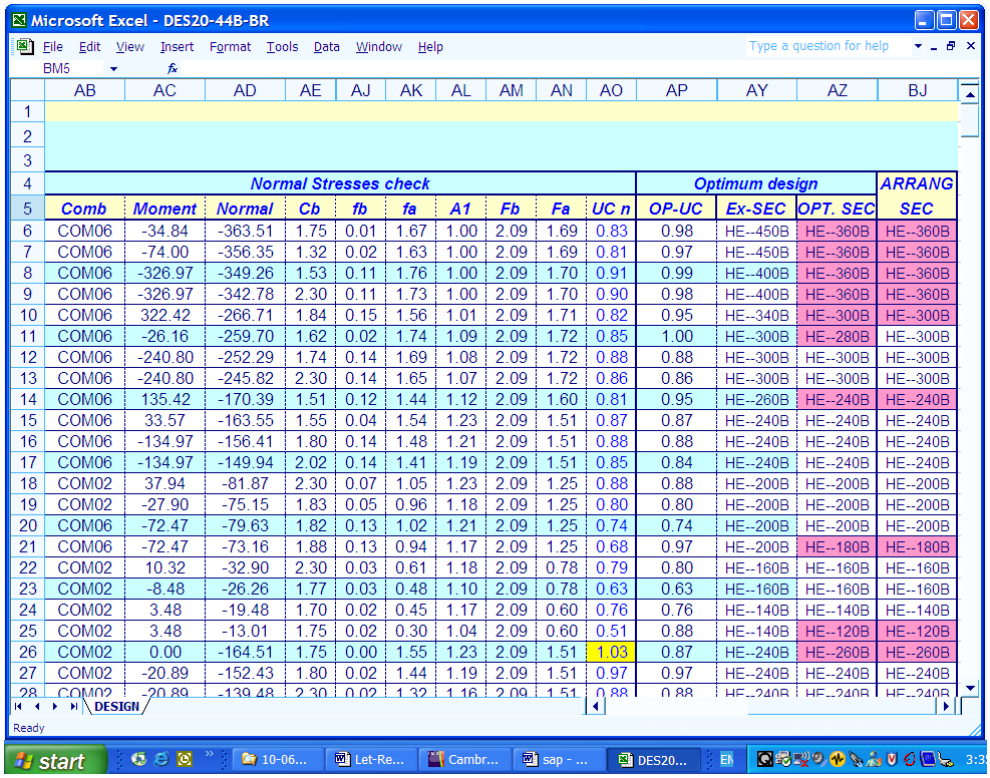

Microsoft Excel - DES20-44B-BR

File Edit View Insert Format Tools Data Window Help — Type a question for help

BM5

				Normal Stresses check							Optimum design			ARRANG
Comb	Moment	Normal	Cb	fb	fa	A1	Fb	Fa	UC n	OP-UC	Ex-SEC	OPT. SEC	SEC	
COM06	-34.84	-363.51	1.75	0.01	1.67	1.00	2.09	1.69	0.83	0.98	HE--450B	HE--360B	HE--360B	
COM06	-74.00	-356.35	1.32	0.02	1.63	1.00	2.09	1.69	0.81	0.97	HE--450B	HE--360B	HE--360B	
COM06	-326.97	-349.26	1.53	0.11	1.76	1.00	2.09	1.70	0.91	0.99	HE--400B	HE--360B	HE--360B	
COM06	-326.97	-342.78	2.30	0.11	1.73	1.00	2.09	1.70	0.90	0.98	HE--400B	HE--360B	HE--360B	
COM06	322.42	-266.71	1.84	0.15	1.56	1.01	2.09	1.71	0.82	0.95	HE--340B	HE--300B	HE--300B	
COM06	-26.16	-259.70	1.62	0.02	1.74	1.09	2.09	1.72	0.85	1.00	HE--300B	HE--280B	HE--300B	
COM06	-240.80	-252.29	1.74	0.14	1.69	1.08	2.09	1.72	0.88	0.88	HE--300B	HE--300B	HE--300B	
COM06	-240.80	-245.82	2.30	0.14	1.65	1.07	2.09	1.72	0.86	0.86	HE--300B	HE--300B	HE--300B	
COM06	135.42	-170.39	1.51	0.12	1.44	1.12	2.09	1.60	0.81	0.95	HE--260B	HE--240B	HE--240B	
COM06	33.57	-163.55	1.55	0.04	1.54	1.23	2.09	1.51	0.87	0.87	HE--240B	HE--240B	HE--240B	
COM06	-134.97	-156.41	1.80	0.14	1.48	1.21	2.09	1.51	0.88	0.88	HE--240B	HE--240B	HE--240B	
COM06	-134.97	-149.94	2.02	0.14	1.41	1.19	2.09	1.51	0.85	0.84	HE--240B	HE--240B	HE--240B	
COM02	37.94	-81.87	2.30	0.07	1.05	1.23	2.09	1.25	0.88	0.88	HE--200B	HE--200B	HE--200B	
COM02	-27.90	-75.15	1.83	0.05	0.96	1.18	2.09	1.25	0.80	0.80	HE--200B	HE--200B	HE--200B	
COM06	-72.47	-79.63	1.82	0.13	1.02	1.21	2.09	1.25	0.74	0.74	HE--200B	HE--200B	HE--200B	
COM06	-72.47	-73.16	1.88	0.13	0.94	1.17	2.09	1.25	0.68	0.97	HE--200B	HE--180B	HE--180B	
COM02	10.32	-32.90	2.30	0.03	0.61	1.18	2.09	0.78	0.79	0.80	HE--160B	HE--160B	HE--160B	
COM02	-8.48	-26.26	1.77	0.03	0.48	1.10	2.09	0.78	0.63	0.63	HE--160B	HE--160B	HE--160B	
COM02	3.48	-19.48	1.70	0.02	0.45	1.17	2.09	0.60	0.76	0.76	HE--140B	HE--140B	HE--140B	
COM02	3.48	-13.01	1.75	0.02	0.30	1.04	2.09	0.60	0.51	0.88	HE--140B	HE--120B	HE--120B	
COM02	0.00	-164.51	1.75	0.00	1.55	1.23	2.09	1.51	1.03	0.87	HE--240B	HE--260B	HE--260B	
COM02	-20.89	-152.43	1.80	0.02	1.44	1.19	2.09	1.51	0.97	0.97	HE--240B	HE--240B	HE--240B	
COM02	-20.89	-139.48	2.30	0.02	1.32	1.16	2.09	1.51	0.88	0.88	HE--240B	HE--240B	HE--240B	

DESIGN

Ready

start 10-06... Let-Re... Cambr... sap - ... DES20... EN 3:3

Figure (3.8) cont.: Sample of Design Output Excel File

3.2.5 Mapping Resulting Relations

The relations between frame height and resulting lateral drift and weight per unit area of the four groups are listed in Tables (3.2) to (3.9) and are illustrated in Figs (3.9) to (3.16). For each group, two tables are presented; the first table presents the values of the top displacement (lateral drift), and the second table presents the values of the weight per unit area of the plan. Values denoted in tables by N/A indicate that the studied case is not applicable. It occurs when the proposed standard sections could not provide sufficient stiffness to optimize lateral drift.

First Group: 3-Bay Frames (12 m Wide):

Table (3.2): Lateral Drift in (cm) for 3-Bay Frames (12 m Wide).

Frame Height (m)	*Rigid Frames*	*Braced Frames*			
		One	*Two*	*Three*	*with Outriggers*
140	N/A	N/A	N/A	28.6	N/A
120	24.5	N/A	N/A	24	N/A
100	20	N/A	20	20	20
80	16	N/A	16	16	16
60	12	12	12	8	12
40	8	8	6	3	5
20	4	1	0.8	0.3	0.5

Table (3.3): Weight in (ton/m^2) for 3-Bay Frames (12 m Wide)

Frame Height (m)	*Rigid Frames*	*Braced Frames*			
		One	*Two*	*Three*	*with Outriggers*
140	N/A	N/A	N/A	8.46	N/A
120	8.48	N/A	N/A	2.88	N/A
100	3.58	N/A	4.85	1.67	6.15
80	2.31	N/A	1.54	0.83	2.96
60	1.29	1.17	0.92	0.54	0.81
40	0.77	0.38	0.31	0.29	0.31
20	0.31	0.13	0.13	0.13	0.13

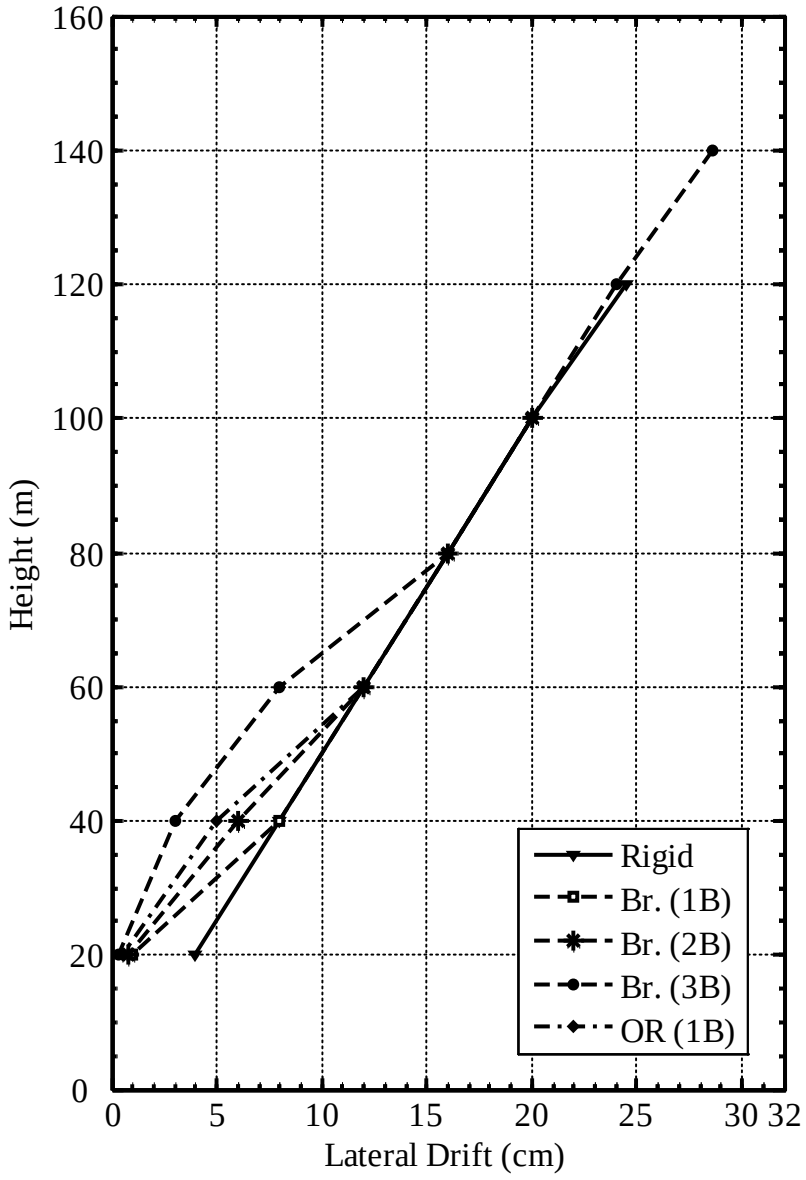

Figure (3.9) : Lateral Drift versus Height for 3-Bay Frames (12 m Wide)

From the lateral drift results shown in Fig.(3.9), it can be seen that deflection controls the design of all rigid frame systems, while it controls the design of one-bay, two-bay, and three-bay braced frames starting from 40, 60, and 80 m height, respectively. Also, deflection controls the design of one-bay braced frames with outrigger truss starting from 60 m height.

It can be seen also that the lateral drift behavior of one-bay braced frames with outrigger truss is almost identical to that with two-bay braced frames

without outrigger truss, and that the lateral drift of braced frames without outrigger truss decreases when the number of braced bays increases.

From the optimum weight results shown in Fig.(3.10), it can be seen that the weight of braced frame system without outrigger truss decreases when the number of braced bays increases. Also, rigid frames produce maximum weights at low heights, while braced frames with outrigger truss produce maximum weights starting from 80 m height.

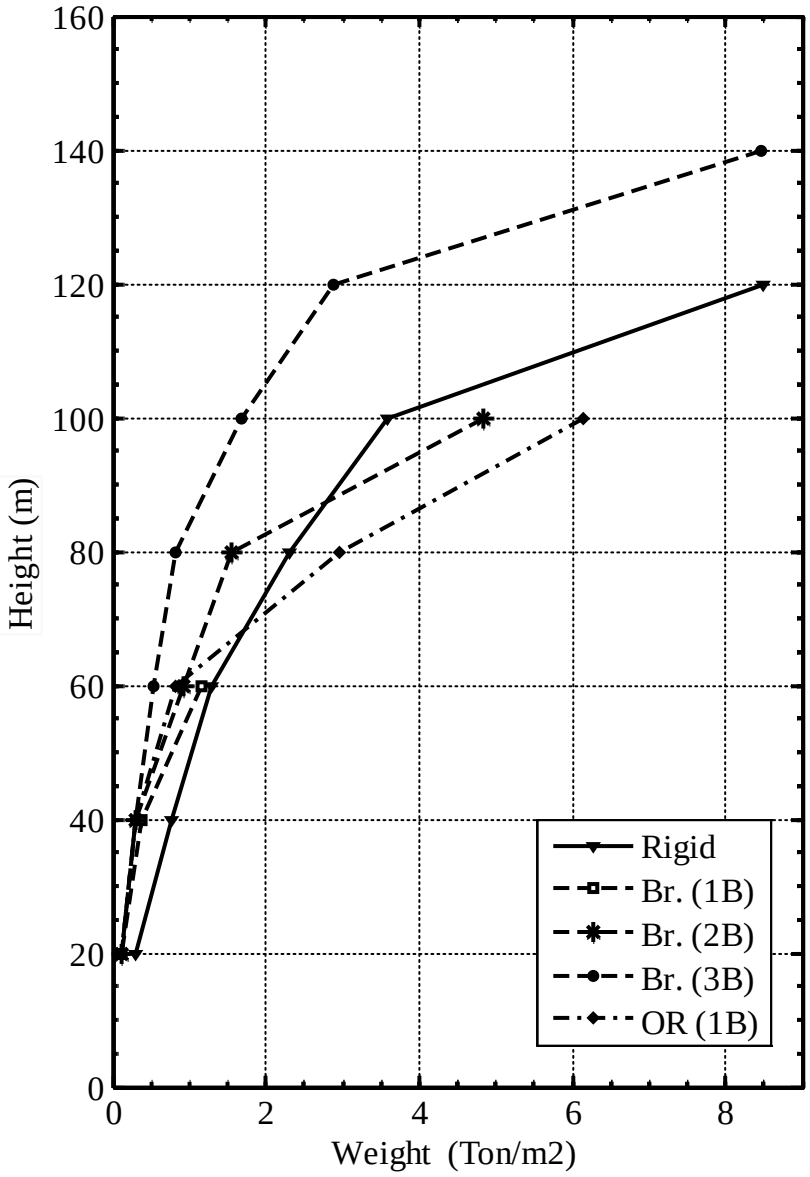

Figure (3.10) : Weight versus Height for 3-Bay Frames (12 m Wide)

Second Group: 4-Bay Frames (16 m Wide):

Table (3.4): Lateral Drift in (cm) for 4-Bay Frames (16 m Wide).

Frame Height (m)	*Rigid Frames*	*Braced Frames*				
		One	*Two*	*Three*	*Four*	*with Outriggers*
160	N/A	N/A	N/A	N/A	32	N/A
152	N/A	N/A	N/A	N/A	30.4	N/A
140	28	N/A	N/A	N/A	28	N/A
120	24	N/A	N/A	24	24	N/A
100	20	N/A	20	20	17	20
80	16	N/A	16	16	10	16
60	12	12	12	10	5	12
40	8	8	4	3.5	2	5
20	4	1	0.5	0.5	0.3	0.5

Table (3.5): Weight in (ton/m^2) for 4-Bay Frames (16 m Wide)

Frame Height (m)	*Rigid Frames*	*Braced Frames*				
		One	*Two*	*Three*	*Four*	*with Outriggers*
160	N/A	N/A	N/A	N/A	4.61	N/A
152	N/A	N/A	N/A	N/A	3.75	N/A
140	6.83	N/A	N/A	N/A	2.81	N/A
120	3.97	N/A	N/A	3.69	1.64	N/A
100	2.78	N/A	2.75	1.92	1.16	5.08
80	1.84	N/A	1.08	0.83	0.78	2.50
60	1.13	0.97	0.52	0.50	0.50	0.73
40	0.72	0.33	0.28	0.28	0.28	0.30
20	0.31	0.12	0.13	0.13	0.13	0.13

From the lateral drift results shown in Fig.(3.11), it can be seen that deflection controls the design of all rigid frame systems, while it controls the design of one-bay, two-bay, three-bay, and four-bay braced frames starting from 40, 60, 80, and 120 m height, respectively. Also, deflection controls the design of one-

bay braced frames with outrigger truss starting from 60 m height.

It can be seen also that the lateral drift behavior of one-bay braced frames with outrigger truss is almost identical to that with two-bay braced frames without outrigger truss, and that the lateral drift of braced frames without outrigger truss decreases when the number of braced bays increases.

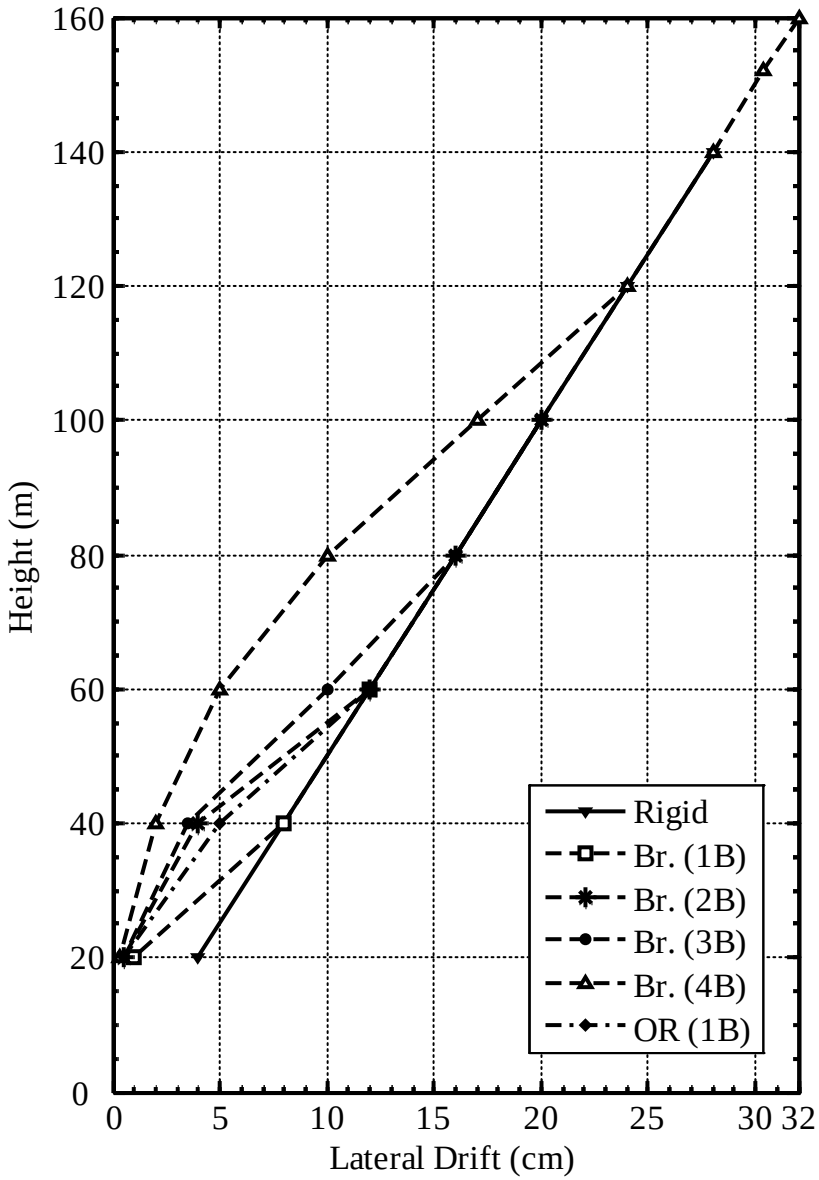

Figure (3.11) : Lateral Drift versus Height for 4-Bay Frames (16 m Wide)

From the optimum weight results shown in Fig.(3.12), it can be seen that the weight of braced frame system without outrigger truss decreases when the number of braced bays increases. Also, rigid frames produce maximum weights at low heights, while braced frames with outrigger truss produce maximum weights starting from 80 m height.

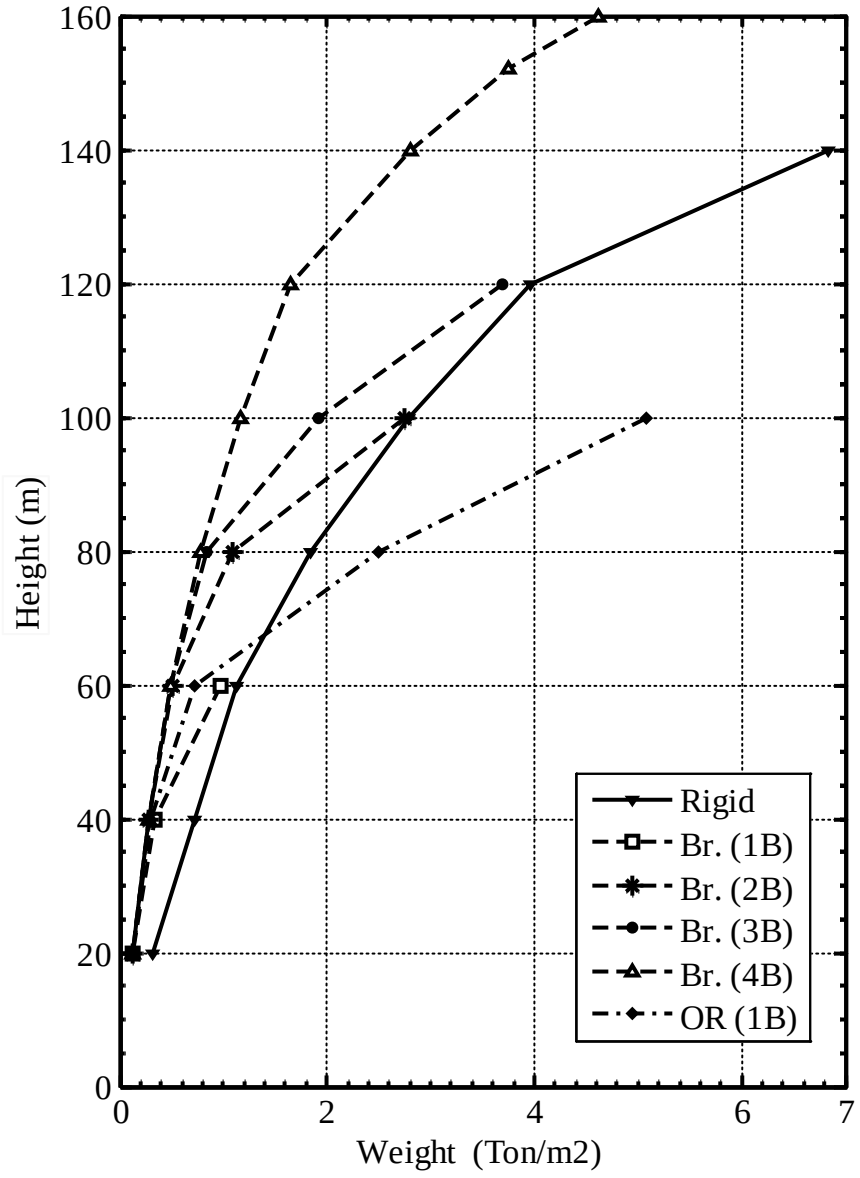

Figure (3.12): Weight versus Height for 4-Bay Frames (16 m Wide)

Third Group: 5-Bay Frames (20 m Wide):

Table (3.6): Lateral Drift in (cm) for 5-Bay Frames (20 m Wide).

Frame Height (m)	*Rigid Frames*	*Braced Frames*					
		One	*Two*	*Three*	*Four*	*Five*	*with Outriggers*
160	32	N/A	N/A	N/A	32	32	N/A
152	30.4	N/A	N/A	N/A	30.4	30.4	N/A
140	28	N/A	N/A	28.6	28	28	N/A
120	24	N/A	N/A	24	24	20	N/A
100	20	N/A	20	20	19	16	20
80	16	N/A	16	13	12	9	16
60	12	12	12	7	6	4	12
40	8	8	4	2	2.5	1.3	4.1
20	4	1	0.5	0.3	0.5	0.3	0.5

Table (3.7): Weight in (ton/m^2) for 5-Bay Frames (20 m Wide)

Frame Height (m)	*Rigid Frames*	*Braced Frames*					
		One	*Two*	*Three*	*Four*	*Five*	*with Outriggers*
160	6.60	N/A	N/A	N/A	5.83	2.90	N/A
152	5.73	N/A	N/A	N/A	4.98	2.48	N/A
140	4.53	N/A	N/A	5.46	3.73	1.85	N/A
120	3.11	N/A	N/A	2.03	2.58	1.40	N/A
100	2.21	N/A	2.35	1.23	1.05	1.00	3.21
80	1.51	N/A	0.98	0.75	0.73	0.71	1.78
60	0.99	0.85	0.48	0.49	0.48	0.46	0.58
40	0.64	0.30	0.28	0.28	0.28	0.28	0.29
20	0.29	0.11	0.11	0.11	0.11	0.11	0.13

From the lateral drift results shown in Fig.(3.13), it can be seen that deflection controls the design of all rigid frame systems, while it controls the design of one-bay, two-bay, three-bay, four-bay, and five-bay braced frames starting from 40, 60, 100, 120, and 140 m height, respectively. Also, deflection

controls the design of one-bay braced frames with outrigger truss starting from 60 m height.

It can be seen also that the lateral drift behavior of one-bay braced frames with outrigger truss is almost identical to that with two-bay braced frames without outrigger truss, and that the lateral drift of braced frames without outrigger truss decreases when the number of braced bays increases.

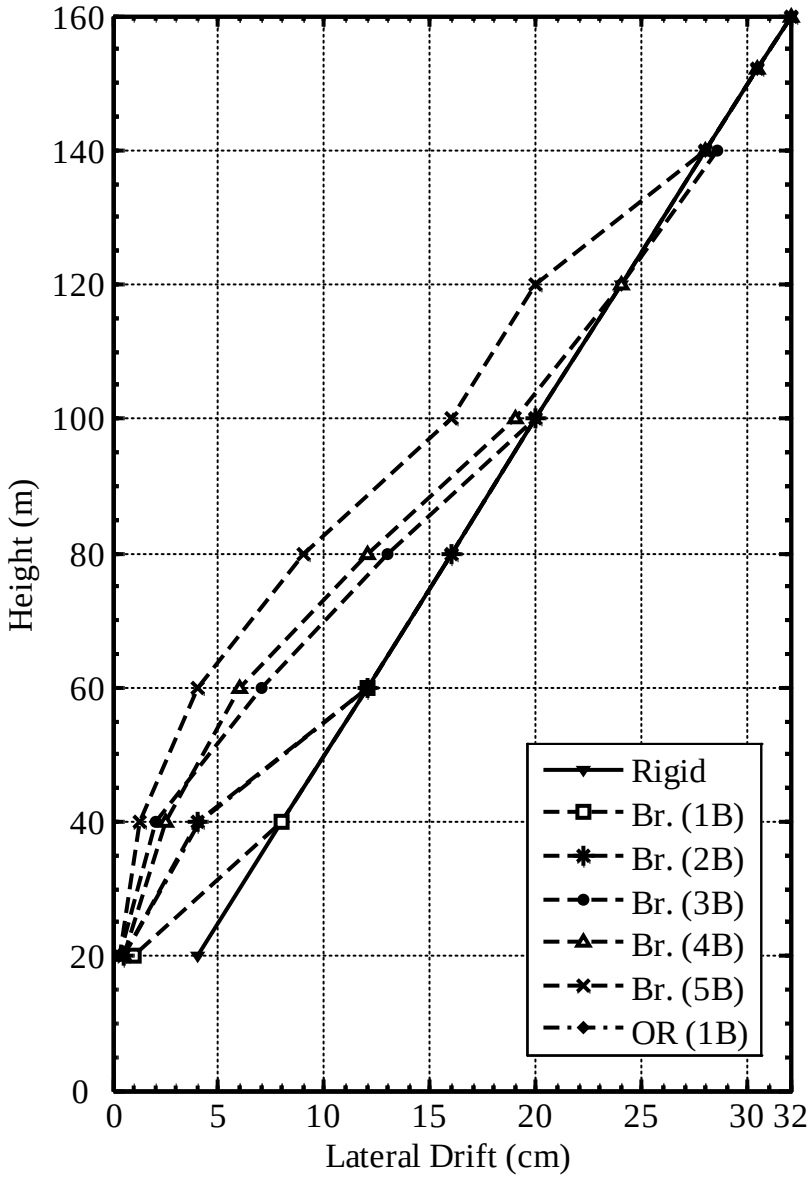

Figure (3.13) : Lateral Drift versus Height for 5-Bay Frames (20 m Wide)

From the optimum weight results shown in Fig.(3.14), it can be seen that the weight of braced frame system without outrigger truss decreases when the number of braced bays increases. Also, rigid frames produce maximum weights at low heights, while braced frames with outrigger truss produce maximum weights starting from 80 m height.

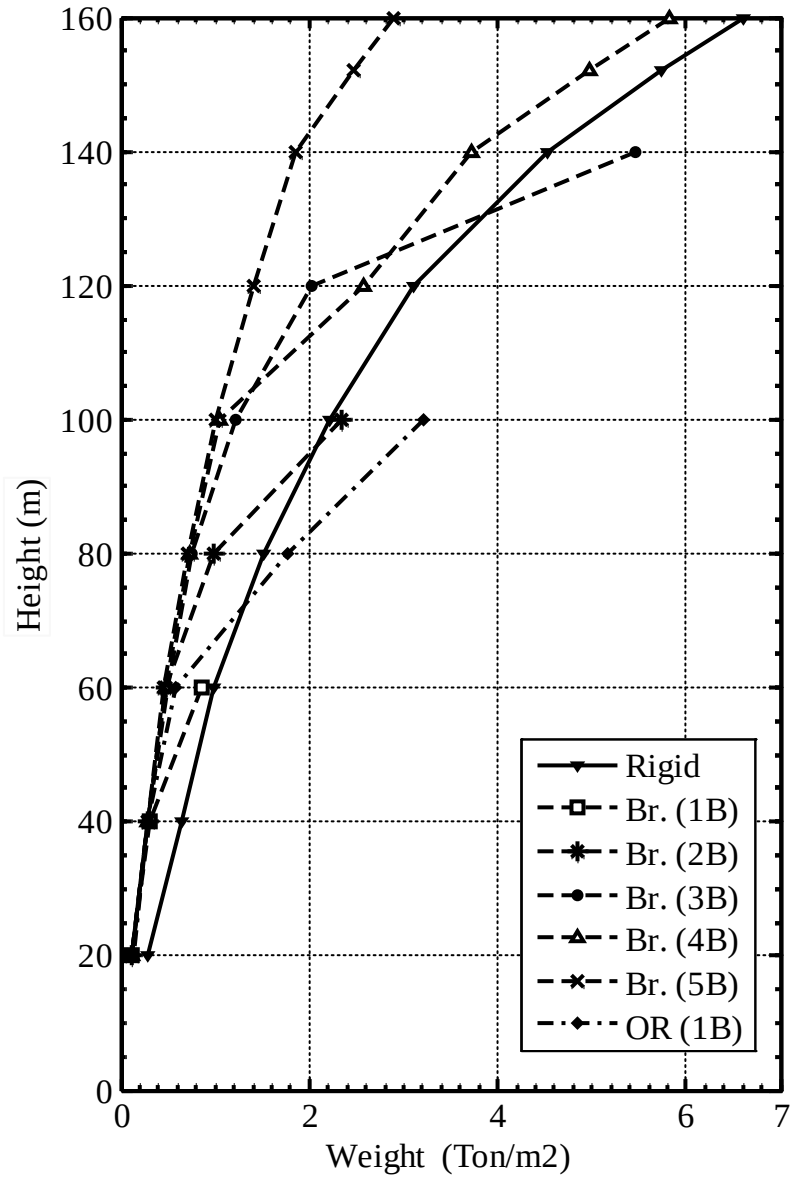

Figure (3.14) : Weight versus Height for 5-Bay Frames (20 m Wide)

Fourth Group: 6-Bay Frames (24 m Wide):

Table (3.8): Lateral Drift in (cm) for 6-Bay Frames (24 m Wide).

Frame Height (m)	*Rigid Frames*	*Braced Frames*						*with Outriggers*	
		One	*Two*	*Three*	*Four*	*Five*	*Six*	*One*	*Two*
160	32	N/A	N/A	N/A	32	32	27	N/A	N/A
152	30.4	N/A	N/A	N/A	30.4	30.4	23	N/A	30.4
140	28	N/A	N/A	28.6	28	28	19	N/A	28
120	24	N/A	N/A	24	22	21	12	N/A	24
100	20	N/A	20	20	13	14	8	20	20
80	16	N/A	16	13	8	9	5	16	11
60	12	12	12	7	3	5	3	12	5
40	8	8	4	2	1.5	2	1	4.3	1.6
20	4	1	0.5	0.3	0.26	0.4	0.2	0.5	0.25

Table (3.9): Weight in (ton/m^2) for 6-Bay Frames (24 m Wide)

Frame Height (m)	*Rigid Frames*	*Braced Frames*						*with Outriggers*	
		One	*Two*	*Three*	*Four*	*Five*	*Six*	*One*	*Two*
160	4.69	N/A	N/A	N/A	3.44	3.33	2.25	N/A	N/A
152	4.20	N/A	N/A	N/A	2.88	2.85	2.10	N/A	8.06
140	3.55	N/A	N/A	4.76	2.19	2.01	1.82	N/A	4.58
120	2.69	N/A	N/A	1.85	1.44	1.38	1.43	N/A	2.43
100	1.99	N/A	2.08	1.17	1.08	1.01	1.06	3.06	1.52
80	1.34	N/A	0.91	0.72	0.74	0.71	0.74	1.85	0.77
60	0.96	0.77	0.46	0.47	0.49	0.47	0.48	0.57	0.49
40	0.51	0.29	0.27	0.26	0.27	0.27	0.27	0.26	0.28
20	0.28	0.10	0.11	0.11	0.11	0.11	0.11	0.11	0.13

From the lateral drift results shown in Fig.(3.15), it can be seen that deflection controls the design of all rigid frame systems, while it controls the design of one-bay, two-bay, three-bay, four-bay, and five-bay braced frames starting from 40, 60, 100, 140, and 140 m height, respectively. Also, deflection

controls the design of one-bay, and two-bay braced frames with outrigger truss starting from 60, and 100 m height, respectively.

It can be seen also that the lateral drift behavior of one-bay braced frames with outrigger truss is almost identical to that with two-bay braced frames without outrigger truss, and two-bay braced frames with outrigger truss is almost identical to that with three-bay braced frames without outrigger truss. In addition to that, the lateral drift of braced frames without outrigger truss decreases when the number of braced bays increases.

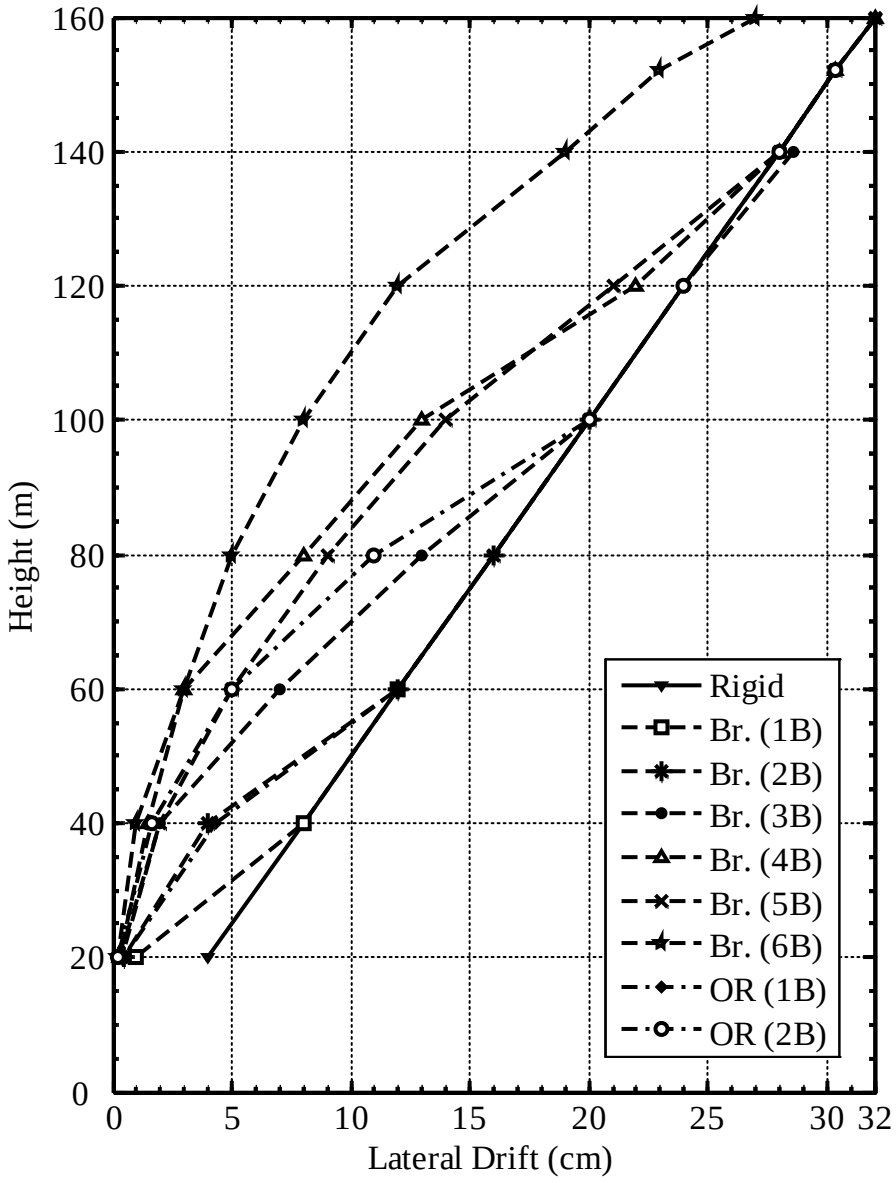

Figure (3.15) : Lateral Drift versus Height for 6-Bay Frames (24 m Wide)

From the optimum weight results shown in Fig.(3.16), it can be seen that the weight of braced frame system without outrigger truss decreases when the number of braced bays increases. Also, rigid frames produce maximum weights at low heights, while braced frames with outrigger truss produce maximum weights starting from 80 m height.

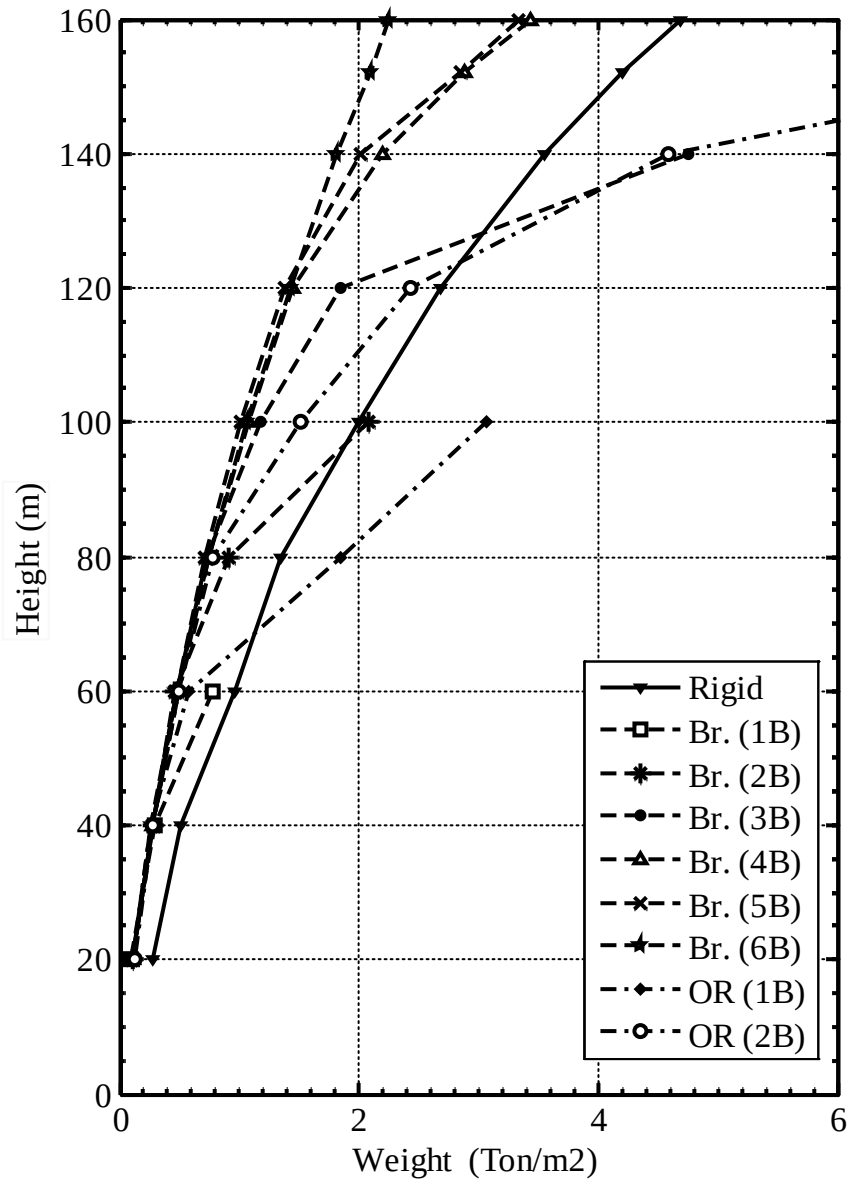

Figure (3.16) : Weight versus Height for 6-Bay Frames (24 m Wide)

3.2.6 Concluding Remarks

From the lateral drift results, it can be observed that deflection controls the design of all rigid frame systems. Deflection also controls the braced frames without outrigger truss when the ratio of the total frame height to the total width of braced bays approaches 7.5 as shown in Fig.(3.17). On the other hand, the strength controls the design of the six-bay braced frames without outrigger.

In addition to that the lateral drift behavior of frames with (n) braced bays with outrigger truss is almost identical to frames with (n+1) braced bays without outrigger truss, where (n) is the number of braced bays.

The results for both lateral drift and weight of rigid frames are generally higher than braced frames systems with few exceptions.

The results for both lateral drift and weight of braced frames without outrigger truss decrease when the number of braced bays increases.

The weight of frames with (n) braced bays with outrigger is higher than that of frames with (n+1) braced bays without outrigger truss.

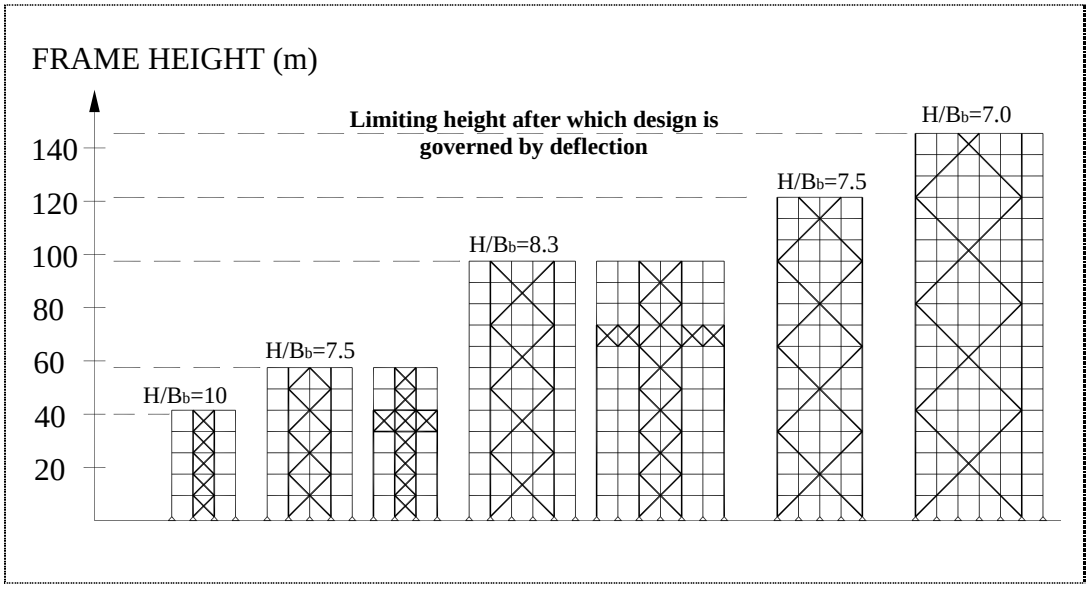

Figure (3.17) Variation of Frame Height Controlling Design with respect to Lateral Load-Resisting System

Figures (3.18) and (3.19) present two samples for the relation of relative weight per unit area versus the lateral load-resisting system at 60 and 80 m heights, respectively. It can be observed that the braced frame system without outrigger truss is the most cost-efficient lateral load resisting system, within the range of studied spans and heights.

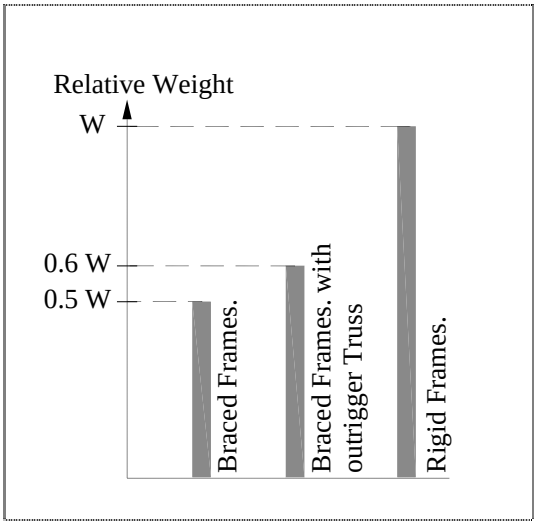

Figure (3.18) Relative Weight / unit area versus Frame Lateral Load-Resisting System at 60 m Height

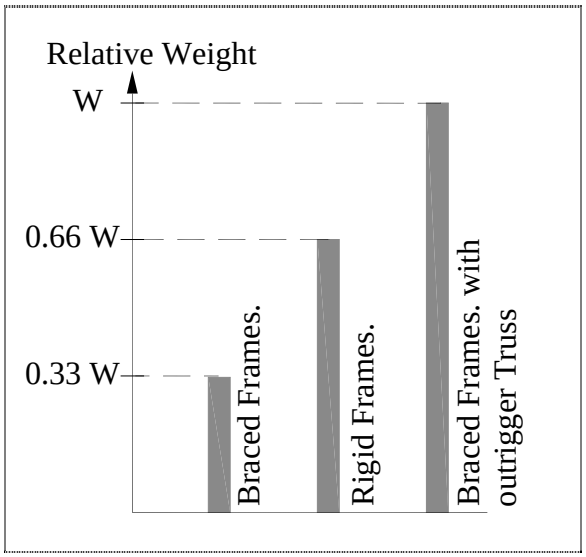

Figure (3.19) Relative Weight / unit area versus Frame Lateral Load-Resisting System at 100 m Height

CHAPTER (4)

ARTIFICIAL NEURAL NETWORK MODEL

The feed-forward backpropagation neural network is the commonly used network for pattern recognition (association or classification), and function approximation problems. Feed-forward networks often have one or more hidden layers of sigmoid neurons followed by an output layer of linear neurons.

4.1 NETWORK SETUP

The architecture of a multilayer network is not completely constrained by the problem to be solved. The number of inputs to the network is constrained by the problem, and the number of neurons in the output layer is constrained by the number of outputs required by the problem. However, the number of layers between network inputs and the output layer and the sizes of the layers are decided from the achieved performance of network.

The number of inputs in the NN will define the frame's dimensions and classify the lateral load-resisting system. There will be two neurons in the output layer to define the lateral drift and optimum weight of frames.

4.1.1 Input and Output Parameters Identification

Input Parameters:

Since the neural network can deal with only numerical parameters, then all the non numerical input parameters has to be identified in a numerical basis. Vector *P* is considered the vector including input parameters of this problem.

$$P = [P_1, P_2, P_3, P_4, P_5]$$

where :

P_1 , defines the total width of the frame in meters, or the number of bays

P_2 , defines the total height of the frame in meters, or the number of stories.

P_3 , identifies the rigid frame systems, it is either zero for non rigid frames or one for rigid frames.

P_4, identifies the braced frame systems, it is either zero for unbraced frames or another value from one to six to describe the number of braced bays.

P_5, identifies the braced frames with outrigger trusses. It is zero for both braced frames and rigid frames and one for braced frames with outrigger trusses.

Figure (4.1) shows three samples of frames with their NN input vector **P**.

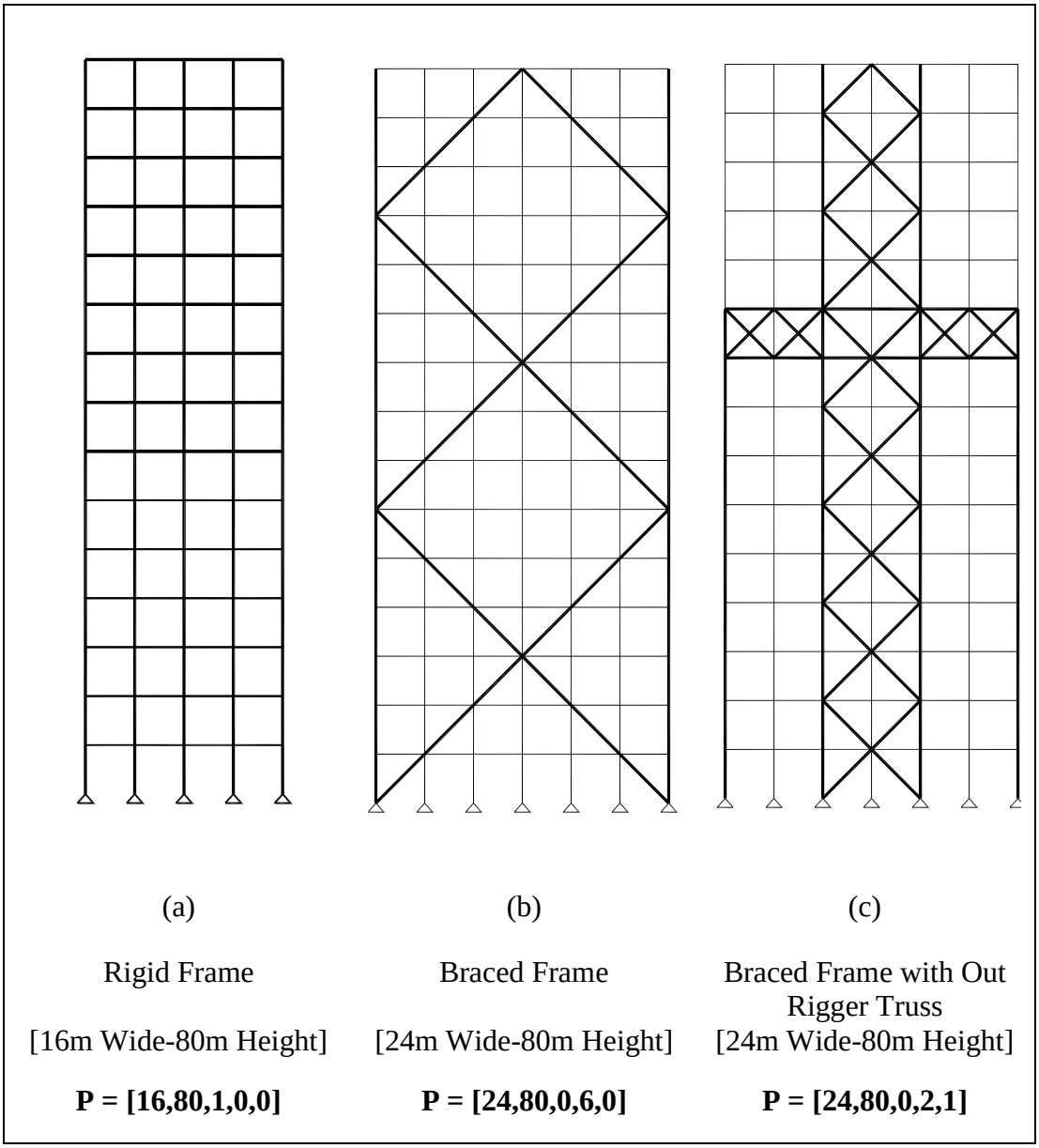

Figure (4.1): Applied Samples of NNs Input Vector P

Output Parameters:

Vector *T* is considered the vector including output targets of this problem.

$$T = [T_1, T_2]$$

where:

T_1, defines the lateral drift in cm

T_2, defines the optimum weight in tone per square meter.

4.1.2 Preprocessing Input and Output data

To enhance the training process of neural network, inputs and targets should be normalized as explained before in item [2.3.9] so that they always fall in a small range.

MATLAB approach for normalizing network inputs and targets is implemented with preprocessing functions. The selected method for preprocessing data is to normalize the mean and standard deviation of the training or testing sets. It normalizes the inputs and targets so that they will have zero mean and unity standard deviation. It implements the following function.

$$X_{i-normal} = (X_i - X_{mean}) / X_{st.dev} \qquad (4.1)$$

4.1.3 Learning Algorithm

There are several different backpropagation training algorithms. They have a variety of different computation and storage requirements, and no one algorithm is best suited to all locations. It is very difficult to know which training algorithm will be the fastest for a given problem. It depends on many factors, including the complexity of the problem, the number of data points in the training sets, the number of weights and biases in the network, the error goal, and whether the network is being used for pattern recognition or function approximation.

The Levenberg-Marquardt algorithm is applied in this problem, because it proved to be the fastest algorithm after several trials of comparison.

4.1.4 Transfer Function

The differentiable sigmoid functions are useful for the neurons of the hidden layers in backpropagation networks. It allows the network to learn nonlinear and linear relationships between input and output vectors.

The tan-sigmoid transfer function shown in Fig.(4.2) takes the input, which may have any value between plus and minus infinity, and squashes the output into the range [-1 to 1].

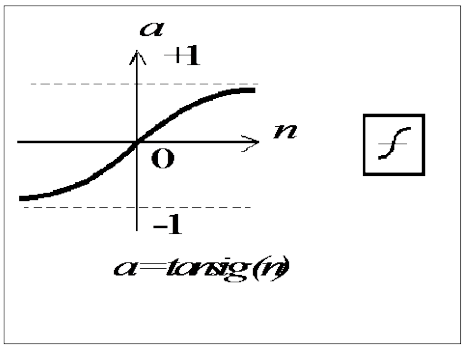

Figure (4.2): Tan-sigmoid Transfer Function

4.1.5 Network Performance

To achieve a proper design of a NN, two approaches will be followed. First, is to minimize the error between network outputs and desired targets. Second, is to ensure that the network is able to generalize, and it is not over fitting.

To minimize the error between outputs and targets, we consider the non dimensional root-mean square error (RMSE) as a measure for the network performance. It is desirable that RMSE reaches to a small value.

$$RMSE = \frac{\sqrt{\frac{\sum_{i=1}^{N}(A_i - T_i)^2}{N}}}{\bar{T}}.100 \qquad (4.2)$$

where A_i is the ith NN output.; T_i is the target for the ith output; N is the number of training or testing sets., and $\bar{T}$ is the target mean value.

To ensure that the NN is able to generalize, we follow the early stopping method in MATLAB for improving generalization. The data is divided into training and testing subsets. The training and testing errors are plotted during the training progress and the training stops when the testing error is increased.

A linear regression between the network outputs and the corresponding targets (training, and testing) is performed, and the correlation coefficient (R) between the network response (A) and the desired target (T) is evaluated. It is desirable that the correlation coefficient (R) approaches to one.

4.1 NETWORK TRAINING AND TESTING PROCESS

The network has been trained with 164 training sets chosen from the performed analysis, and it has been tested with 54 testing sets selected from the plotted charts. Refer to Table (A.1) in annex (A) which lists the training and testing data.

Tables (4.1) and (4.2) summarize the results of training and testing several network architectures. Table (4.1) is for NNs with one hidden layer, while table (4.2) is for NNs with two hidden layers. Each entry in the tables represents not less than 30 different trials, where different random initial weights are used in each trial.

Table (4.1): Performance of NNs with One Hidden Layer

No. of Neurons 1st Layer	*Number Of Iterations*	*Execution Time (sec)*	*Correlation Coefficient (R)*		*(RMSE %)*			
			Drift	*Weight*	*Drift*		*Weight*	
					Train	*Test*	*Train*	*Test*
5	33	0.562	0.9957	0.9863	6.74	5.84	17.82	19.29
6	43	0.734	0.9953	0.9922	7.14	5.93	13.55	14.41
7	45	0.750	0.9954	0.9951	7.09	5.79	10.72	12.03
8	43	0.781	0.9960	0.9969	6.70	5.40	8.22	9.94
9	75	1.266	0.9965	0.9980	6.32	4.74	6.86	7.23
10	54	1.125	0.9967	0.9980	5.97	5.19	6.22	9.04
11	54	1.156	0.9971	0.9981	5.72	4.17	5.89	9.17
12	71	1.594	0.9978	0.9983	4.96	4.09	6.08	7.85
13	74	1.75	0.9979	0.9986	4.82	3.98	5.40	6.81
14	73	1.828	0.9983	0.9986	4.42	3.24	5.38	6.94
15	57	1.656	0.9985	0.9981	3.98	3.45	6.11	8.77

Figure (4.3) shows the relation obtained from Table (4.1) between the overall RMSE for the two output targets versus the number of neurons in NNs with one hidden layer. It is clear from the figure that the average RMSE for both training and testing values approached its minimum value (5.0%) at 14 neurons. Also the minimum RMSE of both training and testing sets are at the same number of neurons, which is the NN with maximum performance and execution time.

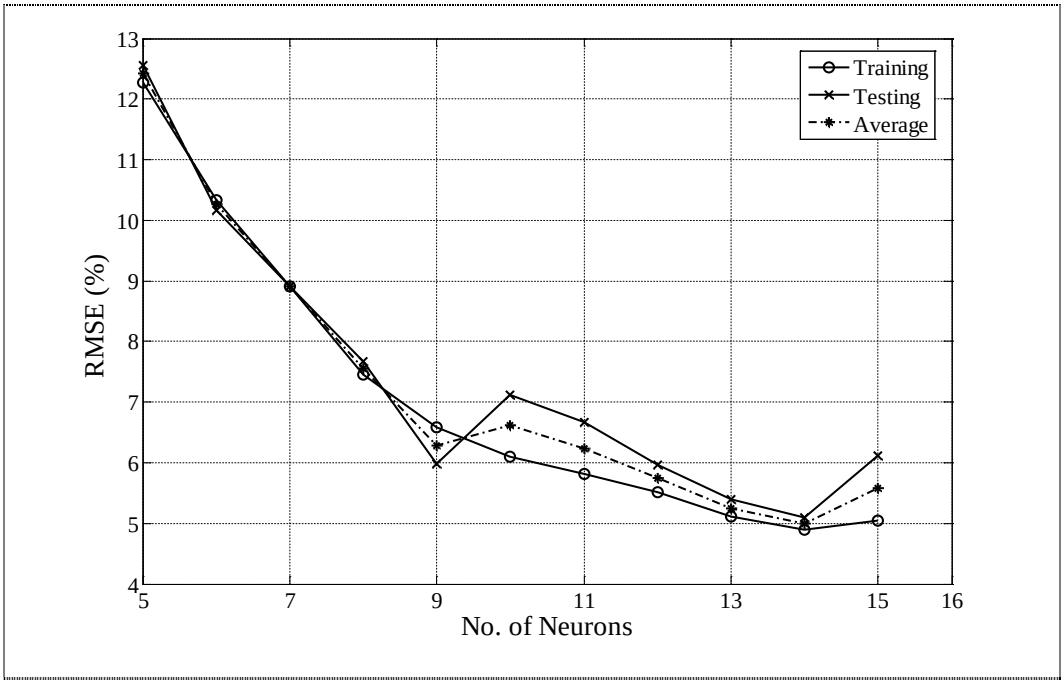

Figure (4.3): RMSE versus No. of Neurons in NNs with One Hidden Layer

Table (4.2): Performance of NNs with Two hidden Layers

No. of Neurons		*No.*	*Execut.*	*Correlation*		*(RMSE %)*			
1st	*2nd*	*Of*	*Time*	*Coefficient (R)*		*Drift*		*Weight*	
Lay.	*Lay.*	*Iterat.*	*(sec)*	*Drift*	*Weight*	*Train*	*Test*	*Train*	*Test*
5	3	48	0.890	0.9959	0.9967	6.61	5.63	8.70	9.89
5	4	60	1.015	0.9963	0.9966	6.34	5.25	8.84	9.59
5	5	53	1.234	0.9974	0.9971	5.39	4.16	8.27	8.84
5	6	118	1.937	0.9980	0.9971	4.82	3.43	6.88	12.10
5	7	73	1.469	0.9987	0.9974	3.58	3.42	7.26	9.73
5	8	95	1.875	0.9983	0.9984	4.29	3.81	5.55	8.12
6	3	107	2.078	0.9976	0.9964	5.09	4.35	9.38	9.53
6	4	97	1.640	0.9985	0.9979	3.85	3.70	6.67	9.05
6	5	142	2.406	0.9980	0.9978	4.70	3.98	6.87	8.95
6	6	74	1.625	0.9983	0.9983	4.25	3.81	5.76	7.93
6	7	66	1.593	0.9985	0.9985	4.07	3.27	5.54	7.35
6	8	80	1.922	0.9988	0.9986	3.40	3.41	5.00	8.00
7	3	143	2.140	0.9973	0.9982	5.42	4.49	6.00	8.40
7	4	82	1.407	0.9976	0.9978	5.02	4.54	6.71	9.12
7	5	64	1.328	0.9981	0.9986	4.47	4.15	5.50	7.39
7	6	80	1.656	0.9986	0.9986	3.81	3.60	5.66	6.15
7	7	61	1.547	0.9982	0.9991	4.24	4.13	4.19	5.70
7	8	74	2.250	0.9990	0.9988	3.24	3.14	4.33	8.19
8	3	56	1.125	0.9979	0.9984	4.44	4.76	5.75	8.01
8	4	50	1.125	0.9988	0.9982	3.33	3.64	4.77	10.56
8	5	57	1.344	0.9989	0.9981	3.30	3.32	6.11	8.78
8	6	68	2.013	0.9989	0.9988	3.41	2.99	4.65	7.50
8	7	63	1.984	0.9993	0.9988	2.66	2.66	4.67	7.49
8	8	45	1.485	0.9990	0.9990	3.43	2.67	4.01	7.19
9	3	109	2.922	0.9989	0.9986	3.30	3.48	5.13	7.90
9	4	75	2.109	0.9992	0.9986	2.89	2.91	5.29	7.56
9	5	76	2.281	0.9992	0.9990	2.87	2.52	3.79	7.20
9	6	75	2.578	0.9993	0.9989	2.66	2.88	3.87	8.10
9	7	47	1.980	0.9990	0.9991	3.14	3.12	3.88	6.84
9	8	47	1.953	0.9988	0.9990	3.63	2.99	3.91	7.31

Table (4.2) cont.: Performance of NNs with Two Hidden Layers

No. of Neurons		*No.*	*Execut.*	*Correlation*		*(RMSE %)*			
1st	*2nd*	*Of*	*Time*	*Coefficient (R)*		*Drift*		*Weight*	
Lay.	*Lay.*	*Iterat..*	*(sec)*	*Drift*	*Weight*	*Train*	*Test*	*Train*	*Test*
10	3	76	1.938	0.9983	0.9990	4.05	4.30	4.61	6.32
10	4	42	1.219	0.9987	0.9988	3.53	3.93	4.74	6.93
10	5	73	2.203	0.9994	0.9991	2.59	2.24	4.14	6.31
10	6	51	1.875	0.9991	0.9990	3.11	2.80	4.25	6.66
10	7	61	2.329	0.9994	0.9991	2.51	2.63	3.46	7.36
11	3	106	2.625	0.9985	0.9984	2.96	5.61	5.25	8.66
11	4	54	1.468	0.9992	0.9989	2.71	3.17	4.52	7.06
11	5	60	1.922	0.9993	0.9990	2.81	2.49	4.29	6.54
11	6	78	3.063	0.9992	0.9992	2.79	2.75	3.83	6.11
12	3	39	1.328	0.9990	0.9988	3.00	3.76	5.10	6.81
12	4	52	1.704	0.9994	0.9991	2.56	2.48	3.76	6.97
12	5	101	3.078	0.9993	0.9994	2.40	3.02	3.09	5.94
13	3	40	1.500	0.9989	0.9990	3.25	3.24	4.21	6.88
13	4	40	1.281	0.9993	0.9987	2.52	2.62	4.76	7.70
13	5	80	3.438	0.99937	0.99911	2.334	2.872	2.667	8.351

Figure (4.4) shows the relation obtained from Table (4.2) between the overall RMSE for the two output targets of training sets versus the number of neurons in NNs with two hidden layers. It can be seen from the figure that the minimum RMSE for training sets is 2.5% resulting from NN [5-13-5-2] with 13 neurons in the first hidden layer and 5 neurons in the second hidden layer. This network performs the training process in 3.44 seconds and 80 iterations.

Figure (4.5) shows the relation obtained from Table (4.2) between the overall RMSE for the two output targets of testing sets versus the number of neurons in NNs with two hidden layers. It can be seen from the figure that the minimum RMSE for testing sets is 4.27% resulting from NN [5-10-5-2] with 10 neurons in the first hidden layer and 5 neurons in the second hidden layer. This network performs the training process in 2.20 seconds and 73 iterations.

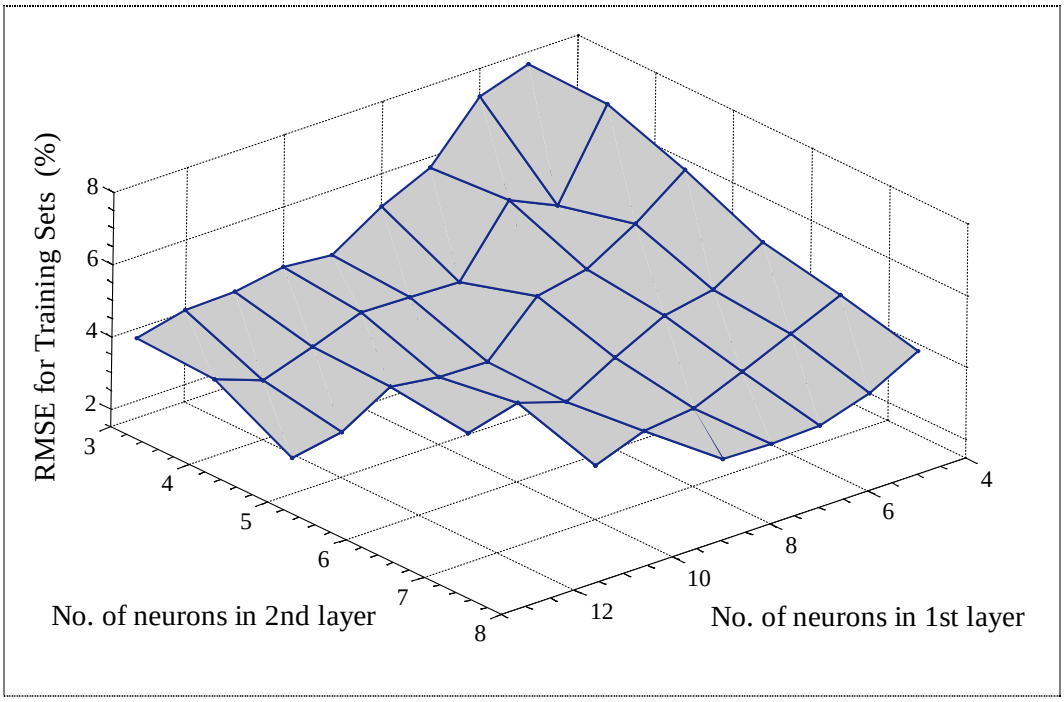

Figure (4.4): RMSE of Training Sets versus No. of Neurons in NNs with Two Hidden Layers

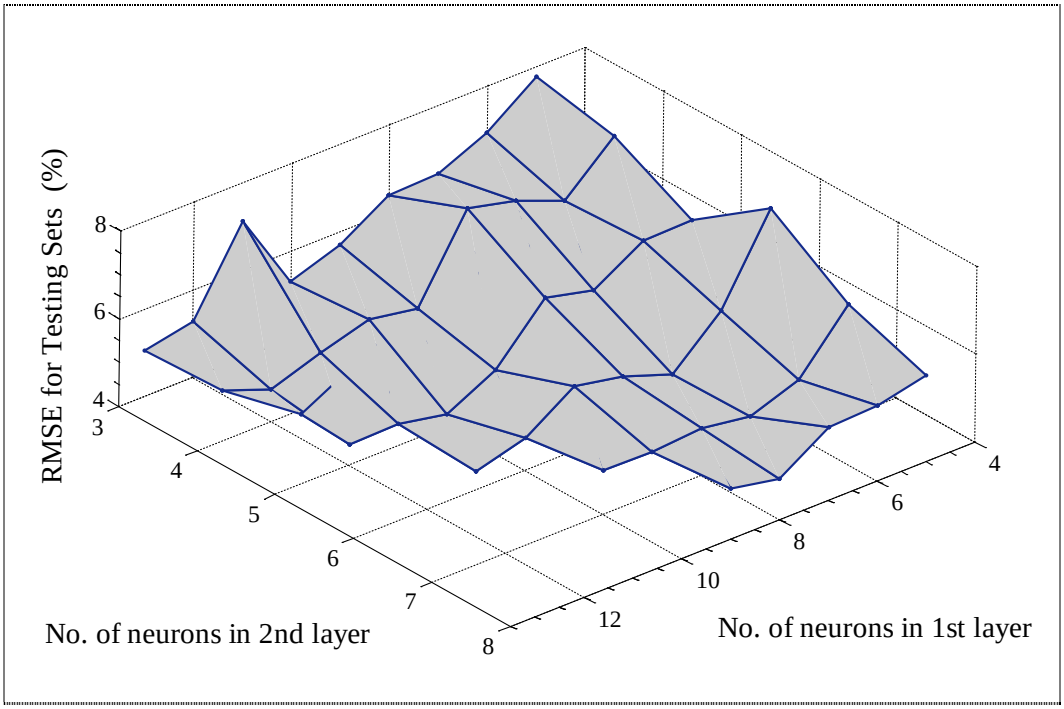

Figure (4.5): RMSE of Testing Sets versus No. of Neurons in NNs with Two Hidden Layers

It is clear then that the minimum RMSE of both training and testing sets do not exist at the same NN.

Figure (4.6) shows the relation obtained from Table (4.2) between the overall average RMSE for training and testing sets versus the number of neurons in NNs with two hidden layers. It can be seen from the figure that the minimum average RMSE is 3.61% resulting from NN [5-12-5-2] with 12 neurons in the first hidden layer and 5 neurons in the second hidden layer. This network performs the training process in 3.08 seconds and 101 iterations.

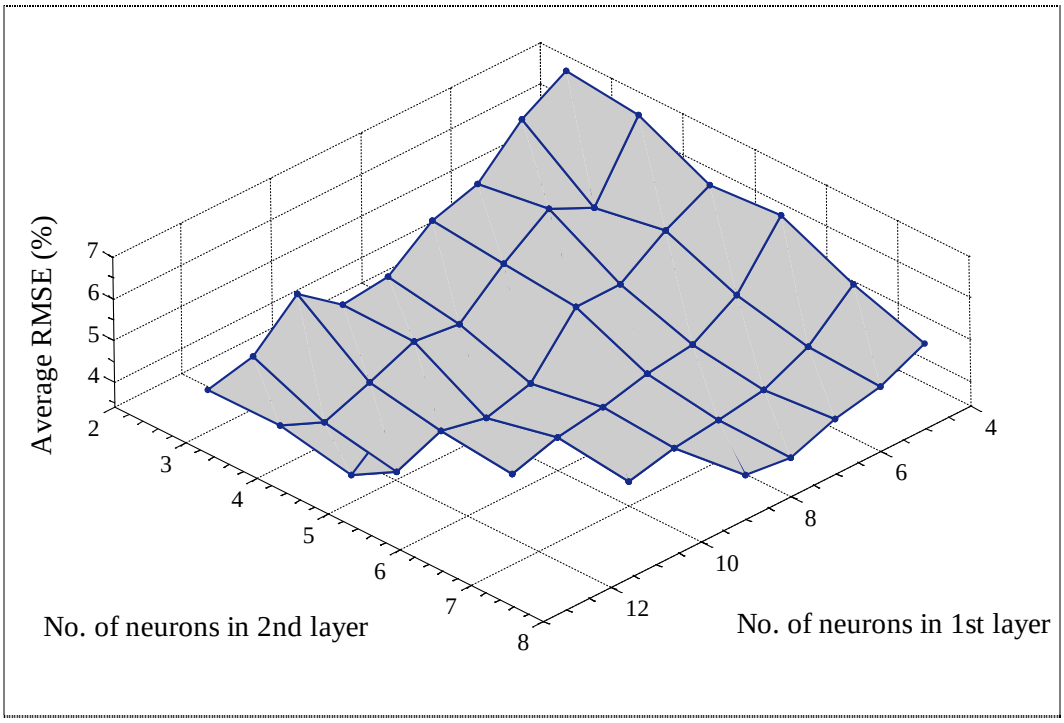

Figure (4.6): Average RMSE for Training and Testing Sets versus No. of Neurons in NNs with Two Hidden Layers

A detailed examination is performed on the performance of the previously mentioned NNs to facilitate the selection of the accepted NN architecture. This is achieved by plotting the training progress and the linear regression of each network.

The training progress of network [5-13-5-2] presented in Fig.(4.7) shows that the RMSE of training and testing sets have not similar characteristics. The RMSE for the training set is driven to a small value with a high rate, while the RMSE of the testing set is not decreasing with the same rate. This indicates that the network is not able to generalize.

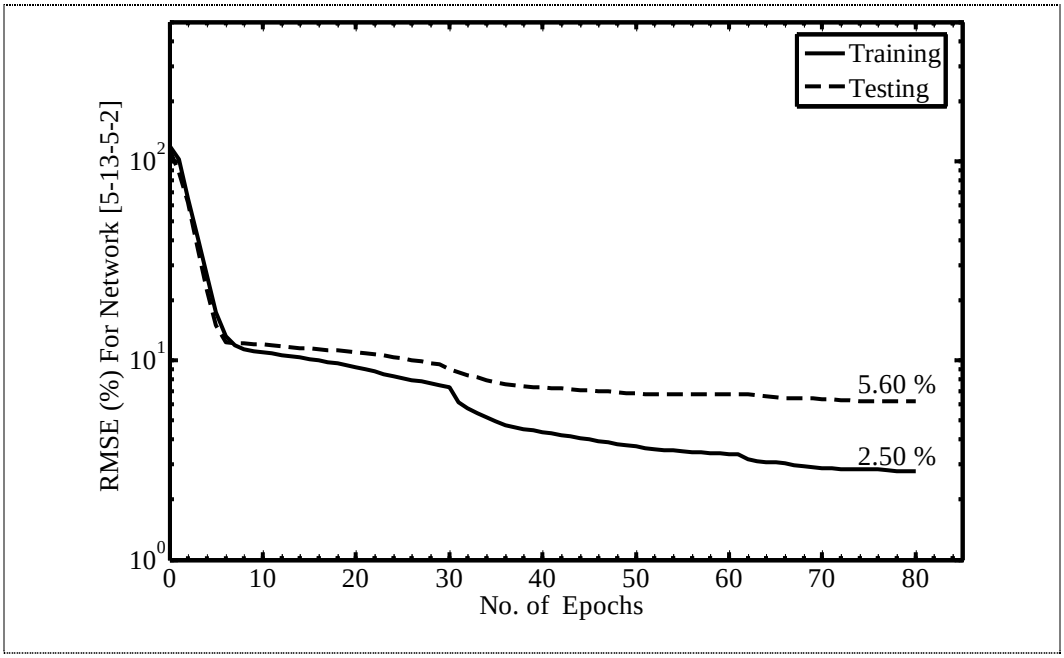

Figure (4.7): Training Plot for Network [5-13-5-2]

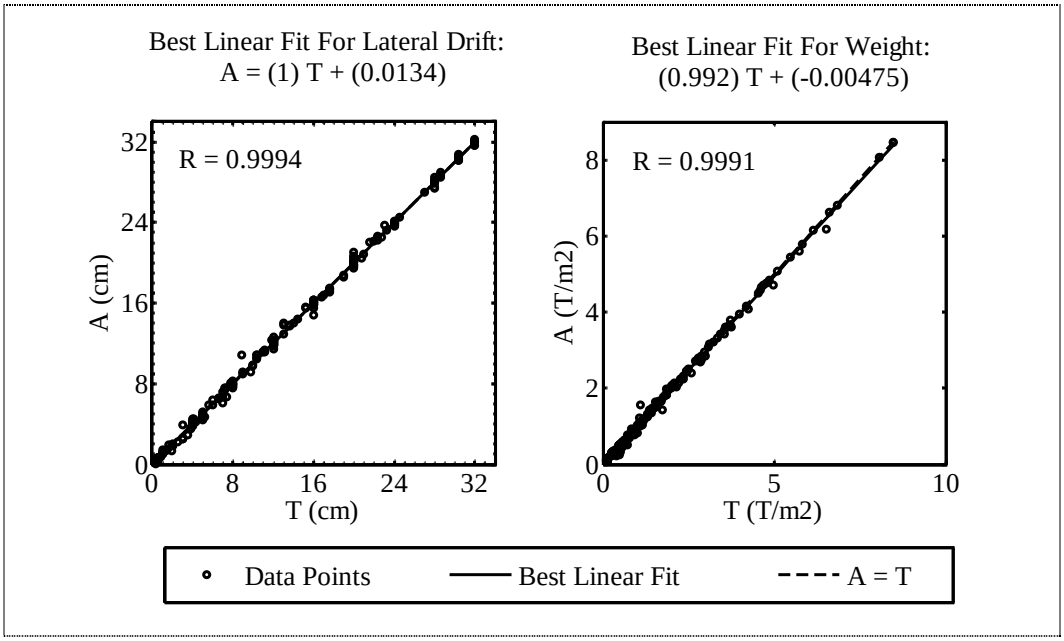

Figure (4.8): Linear Regression for network [5-13-5-2]

The training progress of network [5-10-5-2] presented in Fig.(4.9) shows that the RMSE of training and testing sets have similar characteristics and are close to each other. However Fig.(4.10) shows that the network's correlation coefficients (R) for lateral drift and optimum weight are 0.9994 and 0.9991 respectively. This indicates that the network converges towards one output more than the other.

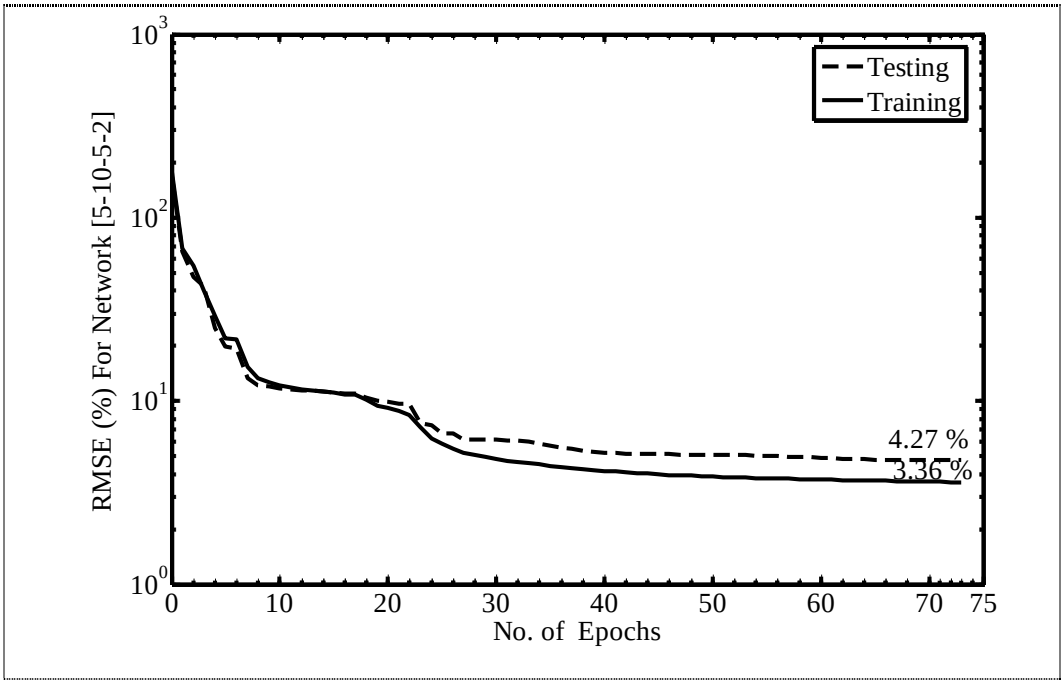

Figure (4.9): Training Plot for Network [5-10-5-2]

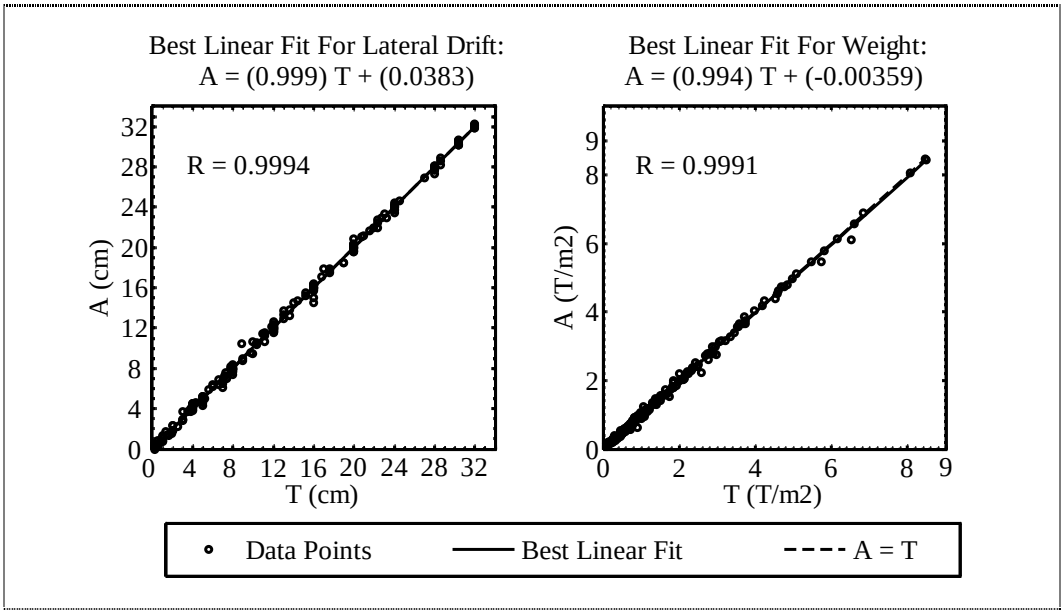

Figure (4.10): Linear Regression for network [5-10-5-2]

The training progress of network [5-12-5-2] presented in Fig.(4.11) shows that the RMSE of training and testing sets have similar characteristics and it doesn't appear that any significant over fitting has occurred. The linear regression presented in Fig.(4.12) shows that the network's correlation coefficients (R) for lateral drift and optimum weight are 0.9993 and 0.9994 respectively. This indicates that the network has approximated the relation quite satisfactorily and it converges towards the two outputs equally.

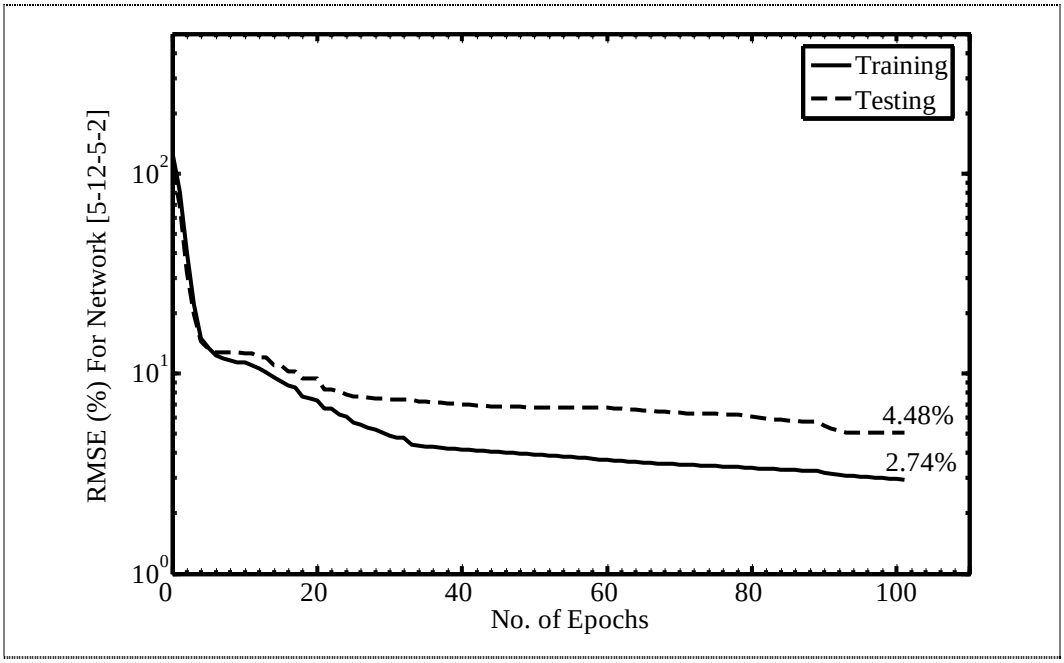

Figure (4.11): Training Plot for Network [5-12-5-2]

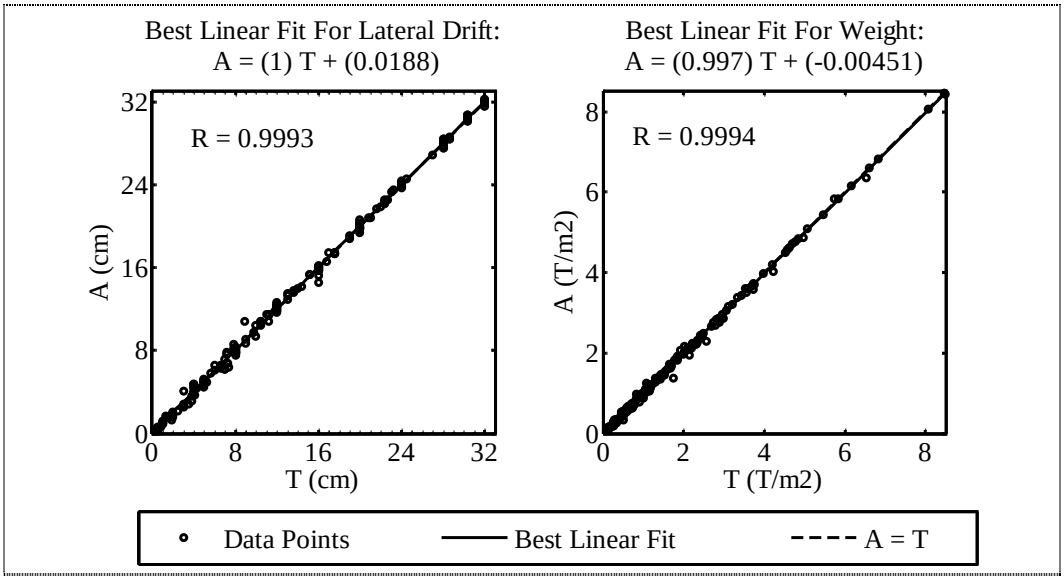

Figure (4.12): Linear Regression for network [5-12-5-2]

4.2 SELECTED NETWORK ARCHITECTURE

After examining the performance of different network architectures, we consider the best network architecture accepted in this investigation is [5-12-5-2]. It is with12 neurons in the first hidden layer and 5 neurons in the second hidden layer. The network proved its ability to track outputs reasonably.

The error during training the network converges within the acceptable limits in 3.08 seconds after 100 iterations. The RMSEs of the first output for training and testing sets are 2.40% and 3.02%, respectively, which is equivalent to an average lateral drift of 0.37 cm. The RMSEs of the second output for training and testing sets are 3.09% and 5.94%, respectively, which is equivalent to an average weight of 0.07 ton/sqm.

CHAPTER (5)

CONCLUSIONS

5.1 Summary

The use of neural network for estimating the maximum lateral drift and optimum weight of different lateral load-resisting systems was investigated. The relation between the frames configurations and their expected lateral drift and weight was mapped by applying the multilayer feed-forward backpropagation artificial neural network. The study involved different configurations for multi-story steel frames under the load combinations of dead, live, and wind loads. The investigation included the optimum design of rigid frames, braced frames and braced frames with single outrigger truss.

Input parameters for network defined the frame configuration in a descriptive numerical form, whereas the output parameters defined the frame maximum lateral drift and expected optimum weight. Networks were trained with the output produced from structural analysis of frames based on finite-element models, and optimum design of elements based on stress and serviceability criteria.

Different architectures of networks were tried to solve the problem. The accepted network architecture was selected based on watching the correlation coefficient resulting from the performed linear regression between the network outputs and the corresponding targets, also based on the non dimensional root-mean square error for both training and testing data.

5.2 Conclusions

Based on the demonstrated investigation, the following characteristics of the studied lateral load-resisting systems and the modeled neural network can be concluded:

- The lateral drift behavior of frames with (n) braced bays with outrigger truss is almost identical to frames with (n+1) braced bays without outrigger truss.

Meanwhile the weight of frames with (n) braced bays with outrigger truss is higher than that of frames with (n+1) braced bays without outrigger truss.

- The braced frame system without outrigger truss is the most cost-efficient lateral load-resisting system, within the range of studied spans and heights.

- From the lateral drift results, it is clear that deflection controls the design of all rigid frame systems, and the braced frames without outrigger truss when the ratio of the total height to the total width of braced bays approaches to 7.5.

- Specifying the parameters of frames under lateral load to a neural network is a time consuming device for the estimation of maximum lateral drift and optimum weight of frames.

- Results of the training process for various architectures of networks with two hidden layers proved better performance than networks with one hidden layer.

- Increasing number of neurons in networks with one hidden layer causes an increase in the execution time. It also improves network performance to a certain limit (up to fourteen neurons) after which the network is not able to generalize. This can be observed in the root mean square error (RMSE) results of testing data.

- Increasing number of neurons in networks with two hidden layers has no specific relation to the execution time, while generally it improves network performance.

- Comparing the (RMSE) results of networks with two hidden layers, we find that, network with twelve neurons in the first hidden layer, and five neurons in the second hidden layer has achieved the optimum performance for the two output targets, however it has the maximum execution time which makes it more expensive than the other networks.

5.3 Future Researches

The research outlined in this thesis may be extended to cover:

- Different ranges of spans and bays.
- Other types of lateral load resisting systems.
- Design governed by other load cases, such as seismic, blast, or differential settlement.

REFERENCES

1. Taranath, B. S., *Structural Analysis and Design of Tall Buildings*, McGraw-Hill, 1988.
2. Liang, Q.Q., Xie, Y.M., and Steven, G.P., "Optimal Topology Design of Bracing Systems for Multistory Steel Frames," *Journal of Structural Engineering*, Vol. 126, No. 7, July 2000, pp. 823-829.
3. "MATLAB Neural network User's Guide," http://www.mathworks.com /access /helpdesk /help /toolbox /nnet, 2004, accessed July, 2005.
4. HBRC, "Egyptian Code of Practice for Steel Constructions and Bridges," *Ministerial Decree No. 279-2001*, Housing and Building Research Centre, 2001.
5. Hoenderkamp, J.C.D., and Bakker, M.C.M., "Analysis of High-rise Braced Frames with Outriggers," *The Structural Design of Tall and Special Buildings*, Vol. 12, No. 4, December 2003, pp. 335-350.
6. "Encyclopedia of Educational Technology (San Diego State University)," http://coe.sdsu.edu/eet/Articles/anns/start.htm, accessed Jan., 2005.
7. Carpenter, W.C., and Barthelemy, J.F., "Common Misconceptions about Neural Networks as Approximators," *Journal of Computing in Civil Engineering*, Vol. 8, No. 3, July 1994, pp. 345-358.
8. Karunanithi, N., Grenney, W. J., Whitley, D., and Bovee, K., "Neural Networks for River Flow Prediction," *Journal of Computing in Civil Engineering*, Vol. 8, No. 2, April 1994, pp. 201-220.
9. Sanchez, L., Arroyo, V., and Garcia, J., "Use of Neural Networks in Design of Coastal Sewage Systems," *Journal of Hydraulic Engineering*, Vol. 124, No. 5, May 1998, pp. 457-464.
10. Gagarin, N., Flood, I., and Albrecht, P., "Computing Truck Attributes with Artificial Neural Networks ," *Journal of Computing in Civil Engineering*, Vol. 8, No. 2, April 1994, pp. 179-200 .
11. Ellis, G. W., Zhao, R., and Penumadu, D., "Stress-Strain Modeling of Sands Using Artificial Neural Networks," *Journal of Geotechnical Engineering*, Vol. 121, No. 5, May 1995, pp. 429-435.

12. Teh, C. I., Wong, K. S., Goh A. T. C., and Jaritngam S., "Prediction of Pile Capacity Using Neural Networks," *Journal of Computing in Civil Engineering*, Vol.11, No. 2, April 1997, pp. 129-138.
13. Mukherjee A., "Self-Organizing Neural Network for Identification of Natural Modes," *Journal of Computing in Civil Engineering*, Vol. 11, No. 1, January 1997, pp. 74-77.
14. Zhao, J., Ivan, J. N., and DeWolf, J. T., "Structural Damage Detection Using Artificial Neural Networks," *Journal of Infrastructure Systems*, Vol. 4, No. 3, September 1998, pp. 93-101.
15. Xu, B., Wu, Z. S., and Yokoyama, K., "Neural Networks for Decentralized Control of Cable-Stayed Bridge," *Journal of Bridge Engineering*, Vol. 8, No. 4, July/August 2003, pp. 229-236.
16. Moheeeb, E. I., "Neural Network for Predicting Price Per Square Meter of Concrete Building Projects," M Sc. Thesis, Cairo University, 2004.
17. Ezeldin, A. S., and Sharara, L. M., "Neural Networks for Estimating the Productivity of Concreting Activities," *Journal of Construction Engineering and Management*, Vol. 132, No. 6, June 2006, pp. 650-656.
18. Yeh, I., "Exploring Concrete Slump Model using Artificial Neural Networks," *Journal of Computing in Civil Engineering*, Vol. 20, No. 3, May/June 2006, pp. 217-221.
19. Sherif, A. M., "Application of Artificial Neural Networks to the assessment of Building Irregularity effects on the Seismic Response," M Sc. Thesis, Cairo University, 1998.
20. Mukherjee, A., Deshpande, J.M., and Anmala, J., "Prediction of Buckling Load of Columns using Artificial Neural Networks," *Journal of Structural Engineering*, Vol. 122, No. 11, November 1996, pp. 1385-1387.
21. Adeli, H., and Karim, A., "Neural Network Model for Optimization of Cold-Formed Steel Beams," *Journal of Structural Engineering*, Vol. 123, No. 11, November 1997, pp. 1535-1543.
22. Chuang, P. H., Goh, A. T. C., and Wu X., "Modeling the Capacity of Pin-Ended Slender Reinforced Concrete Columns Using Neural Networks," *Journal of Structural Engineering*, Vol. 124, No. 7, July 1998, pp. 830-838.

23. Sanad, A., and Saka M. P., “Shear Strength of Reinforced-Concrete Deep Beams using Neural Networks ,” *Journal of Structural Engineering*, Vol. 127, No. 7, July 2001, pp. 818-828.
24. Demirtas B., De Santiago E., and O’leary J. R., “Classification of Steel Semi-Rigid Connections by Neural Networks,” Proc. of the 2004 Structures Congress, Nashville, Tennessee, May 2004.
25. Wilson, E. L.,“SAP(2000) Users Manual”, Copyright Computer and Structures, Inc, 1978-2004.
26. “Learning MATLAB,” http://www.mathworks.com/academia/student_version /doc_r14.html, accessed January, 2004.

Annex (A)

Table (A.1): Input and Output Training Data

No.	*Frame Configurations*					Lateral Drift (cm)	Weight (Ton/sqm)
	Geometry		*Systems*				
	width (m)	*height (m)*	*fixed*	*braced bays*	*out rigger*		
1	12	120	1	0	0	24.5	8.48
2	12	100	1	0	0	20	3.58
3	12	80	1	0	0	16	2.31
4	12	60	1	0	0	12	1.29
5	12	40	1	0	0	8	0.77
6	12	20	1	0	0	4	0.31
7	12	60	0	1	0	12	1.17
8	12	40	0	1	0	8	0.38
9	12	20	0	1	0	1	0.13
10	12	100	0	2	0	20	4.85
11	12	80	0	2	0	16	1.54
12	12	60	0	2	0	12	0.92
13	12	40	0	2	0	6	0.31
14	12	20	0	2	0	0.8	0.13
15	12	140	0	3	0	28.6	8.46
16	12	120	0	3	0	24	2.88
17	12	100	0	3	0	20	1.67
18	12	80	0	3	0	16	0.83
19	12	60	0	3	0	8	0.54
20	12	40	0	3	0	3	0.29
21	12	20	0	3	0	0.3	0.13
22	12	100	0	1	1	20	6.15
23	12	80	0	1	1	16	2.96
24	12	60	0	1	1	12	0.81
25	12	40	0	1	1	5	0.31
26	12	20	0	1	1	0.5	0.13
27	16	140	1	0	0	28	6.83
28	16	120	1	0	0	24	3.97

Table (A.1) cont.: Input and Output Training Data

No.	*Frame Configurations*					Lateral Drift (cm)	Weight (Ton/sqm)
	Geometry		*Systems*				
	width (m)	*height (m)*	*fixed*	*braced bays*	*out rigger*		
29	16	100	1	0	0	20	2.78
30	16	80	1	0	0	16	1.84
31	16	60	1	0	0	12	1.13
32	16	40	1	0	0	8	0.72
33	16	20	1	0	0	4	0.31
34	16	60	0	1	0	12	0.97
35	16	40	0	1	0	8	0.33
36	16	20	0	1	0	1	0.12
37	16	100	0	2	0	20	2.75
38	16	80	0	2	0	16	1.08
39	16	60	0	2	0	12	0.52
40	16	40	0	2	0	4	0.28
41	16	20	0	2	0	0.5	0.13
42	16	120	0	3	0	24	3.69
43	16	100	0	3	0	20	1.92
44	16	80	0	3	0	16	0.83
45	16	60	0	3	0	10	0.50
46	16	40	0	3	0	3.5	0.28
47	16	20	0	3	0	0.5	0.13
48	16	160	0	4	0	32	4.61
49	16	140	0	4	0	28	2.81
50	16	120	0	4	0	24	1.64
51	16	100	0	4	0	17	1.16
52	16	80	0	4	0	10	0.78
53	16	60	0	4	0	5	0.50
54	16	40	0	4	0	2	0.28
55	16	20	0	4	0	0.3	0.13
56	16	100	0	1	1	20	5.08
57	16	80	0	1	1	16	2.50
58	16	60	0	1	1	12	0.73
59	16	40	0	1	1	5	0.30

Table (A.1) cont.: Input and Output Training Data

No.	*Frame Configurations*					Lateral Drift (cm)	Weight (Ton/sqm)
	Geometry		*Systems*				
	width (m)	*height (m)*	*fixed*	*braced bays*	*out rigger*		
60	16	20	0	1	1	0.5	0.13
61	20	160	1	0	0	32	6.60
62	20	140	1	0	0	28	4.53
63	20	120	1	0	0	24	3.11
64	20	100	1	0	0	20	2.21
65	20	80	1	0	0	16	1.51
66	20	60	1	0	0	12	0.99
67	20	40	1	0	0	8	0.64
68	20	20	1	0	0	4	0.29
69	20	60	0	1	0	12	0.85
70	20	40	0	1	0	8	0.30
71	20	20	0	1	0	1	0.11
72	20	100	0	2	0	20	2.35
73	20	80	0	2	0	16	0.98
74	20	60	0	2	0	12	0.48
75	20	40	0	2	0	4	0.28
76	20	20	0	2	0	0.5	0.11
77	20	140	0	3	0	28.6	5.46
78	20	120	0	3	0	24	2.03
79	20	100	0	3	0	20	1.23
80	20	80	0	3	0	13	0.75
81	20	60	0	3	0	7	0.49
82	20	40	0	3	0	2	0.28
83	20	20	0	3	0	0.3	0.11
84	20	160	0	4	0	32	5.83
85	20	140	0	4	0	28	3.73
86	20	120	0	4	0	24	2.58
87	20	100	0	4	0	19	1.05
88	20	80	0	4	0	12	0.73
89	20	60	0	4	0	6	0.48
90	20	40	0	4	0	2.5	0.28

Table (A.1) cont.: Input and Output Training Data

No.	*Frame Configurations*					Lateral Drift (cm)	Weight (Ton/sqm)
	Geometry		*Systems*				
	width (m)	*height (m)*	*fixed*	*braced bays*	*out rigger*		
91	20	20	0	4	0	0.5	0.11
92	20	160	0	5	0	32	2.90
93	20	140	0	5	0	28	1.85
94	20	120	0	5	0	20	1.40
95	20	100	0	5	0	16	1.00
96	20	80	0	5	0	9	0.71
97	20	60	0	5	0	4	0.46
98	20	40	0	5	0	1.3	0.28
99	20	20	0	5	0	0.3	0.11
100	20	100	0	1	1	20	3.21
101	20	80	0	1	1	16	1.78
102	20	60	0	1	1	12	0.58
103	20	40	0	1	1	4.1	0.29
104	20	20	0	1	1	0.5	0.13
105	24	160	1	0	0	32	4.69
106	24	140	1	0	0	28	3.55
107	24	120	1	0	0	24	2.69
108	24	100	1	0	0	20	1.99
109	24	80	1	0	0	16	1.34
110	24	60	1	0	0	12	0.96
111	24	40	1	0	0	8	0.51
112	24	20	1	0	0	4	0.28
113	24	60	0	1	0	12	0.77
114	24	40	0	1	0	8	0.29
115	24	20	0	1	0	1	0.10
116	24	100	0	2	0	20	2.08
117	24	80	0	2	0	16	0.91
118	24	60	0	2	0	12	0.46
119	24	40	0	2	0	4	0.27
120	24	20	0	2	0	0.5	0.11

Table (A.1) cont.: Input and Output Training Data

No.	*Frame Configurations*					Lateral Drift (cm)	Weight (Ton/sqm)
	Geometry		*Systems*				
	width (m)	*height (m)*	*fixed*	*braced bays*	*out rigger*		
121	24	140	0	3	0	28.6	4.76
122	24	120	0	3	0	24	1.85
123	24	100	0	3	0	20	1.17
124	24	80	0	3	0	13	0.72
125	24	60	0	3	0	7	0.47
126	24	40	0	3	0	2	0.26
127	24	20	0	3	0	0.3	0.11
128	24	160	0	4	0	32	3.44
129	24	140	0	4	0	28	2.19
130	24	120	0	4	0	22	1.44
131	24	100	0	4	0	13	1.08
132	24	80	0	4	0	8	0.74
133	24	60	0	4	0	3	0.49
134	24	40	0	4	0	1.5	0.27
135	24	20	0	4	0	0.26	0.11
136	24	160	0	5	0	32	3.33
137	24	140	0	5	0	28	2.01
138	24	120	0	5	0	21	1.38
139	24	100	0	5	0	14	1.01
140	24	80	0	5	0	9	0.71
141	24	60	0	5	0	5	0.47
142	24	40	0	5	0	2	0.27
143	24	20	0	5	0	0.4	0.11
144	24	160	0	6	0	27	2.25
145	24	140	0	6	0	19	1.82
146	24	120	0	6	0	12	1.43
147	24	100	0	6	0	8	1.06
148	24	80	0	6	0	5	0.74
149	24	60	0	6	0	3	0.48
150	24	40	0	6	0	1	0.27
151	24	20	0	6	0	0.2	0.11

Table (A.1) cont.: Input and Output Training Data

No.	*Frame Configurations*					Lateral Drift (cm)	Weight (Ton/sqm)
	Geometry		*Systems*				
	width (m)	*height (m)*	*fixed*	*braced bays*	*out rigger*		
152	24	100	0	1	1	20	3.06
153	24	80	0	1	1	16	1.85
154	24	60	0	1	1	12	0.57
155	24	40	0	1	1	4.3	0.26
156	24	20	0	1	1	0.5	0.11
157	24	152	0	2	1	30.4	8.06
158	24	140	0	2	1	28	4.58
159	24	120	0	2	1	24	2.43
160	24	100	0	2	1	20	1.52
161	24	80	0	2	1	11	0.77
162	24	60	0	2	1	5	0.49
163	24	40	0	2	1	1.6	0.28
164	24	20	0	2	1	0.25	0.13

Table (A.2): Input and Output Testing Data

No.	*Frame Configurations*					Lateral Drift (cm)	Weight (Ton/sqm)
	Geometry		*Systems*				
	width (m)	*height (m)*	*fixed*	*braced bays*	*out rigger*		
1	12	112	1	0	0	22.7	6.52
2	12	52	1	0	0	10.4	1.08
3	12	56	0	1	0	11.2	1.01
4	12	36	0	1	0	6.6	0.33
5	12	76	0	2	0	15.2	1.42
6	12	36	0	2	0	4.96	0.28
7	12	108	0	3	0	21.6	2.15
8	12	68	0	3	0	11.2	0.66
9	12	88	0	1	1	17.6	4.23
10	12	48	0	1	1	7.8	0.51
11	16	116	1	0	0	23.2	3.73
12	16	56	1	0	0	11.2	1.04
13	16	52	0	1	0	10.4	0.71
14	16	32	0	1	0	5.2	0.24
15	16	88	0	2	0	17.6	1.75
16	16	48	0	2	0	7.2	0.38
17	16	112	0	3	0	22.4	2.98
18	16	52	0	3	0	7.4	0.41
19	16	152	0	4	0	30.4	3.75
20	16	72	0	4	0	8	0.67
21	16	88	0	1	1	17.6	3.53
22	16	48	0	1	1	7.8	0.47
23	20	152	1	0	0	30.4	5.73
24	20	72	1	0	0	14.4	1.30
25	20	52	0	1	0	10.4	0.63
26	20	28	0	1	0	3.8	0.19
27	20	76	0	2	0	15.2	0.88
28	20	44	0	2	0	5.6	0.32
29	20	112	0	3	0	22.4	1.71

Table (A.2) cont.: Input and Output Testing Data

No.	*Frame Configurations*					Lateral Drift (cm)	Weight (Ton/sqm)
	Geometry		*Systems*				
	width (m)	*height (m)*	*fixed*	*braced bays*	*out rigger*		
30	20	76	0	3	0	11.8	0.70
31	20	152	0	4	0	30.4	4.98
32	20	64	0	4	0	7.2	0.53
33	20	152	0	5	0	30.4	2.48
34	20	72	0	5	0	7	0.61
35	20	88	0	1	1	17.6	2.35
36	20	48	0	1	1	7.26	0.40
37	24	152	1	0	0	30.4	4.20
38	24	88	1	0	0	17.6	1.60
39	24	52	0	1	0	10.4	0.58
40	24	36	0	1	0	6.6	0.25
41	24	68	0	2	0	13.6	0.64
42	24	28	0	2	0	1.9	0.18
43	24	104	0	3	0	20.8	1.30
44	24	44	0	3	0	3	0.30
45	24	152	0	4	0	30.4	2.88
46	24	64	0	4	0	4	0.54
47	24	152	0	5	0	30.4	2.85
48	24	108	0	5	0	16.8	1.16
49	24	152	0	6	0	23	2.10
50	24	68	0	6	0	3.8	0.58
51	24	68	0	1	1	13.6	1.09
52	24	52	0	1	1	8.92	0.45
53	24	112	0	2	1	22.4	2.06
54	24	76	0	2	1	9.8	0.71